



The Dwarf Blue Compact Galaxies

Jean Audouze, Michel Dennefeld and Daniel Kunth,
Institut d'Astrophysique du CNRS, Paris

1. Introduction

Among the very different types of galaxies which can be analysed, the dwarf blue compact galaxies have been first recognized as a class by Sargent and Searle (1970: *Astrophysical Journal*, **162**, 455). Some important properties let them be priceless tools to enlighten many basic astrophysical problems, such as the primordial nucleosynthesis and cosmology, the chemical evolution of galaxies and the theories of star formation. These galaxies are generally dwarf irregular objects with low mass but the bulk of the luminosity is in the blue range. Their spectra look strikingly like those of a giant HII region. That is why they have been called extragalactic HII region by Sargent and Searle. From their emission lines it is rather straightforward to derive their He, N, O, Ne and possibly S content. Some of these abundances, including some of our own results obtained at La Silla, are summarized in Section 3.

Finally we will show the most important implications of results deduced from the study of these galaxies:

(i) Their weak metallicity can be correlated with their high atomic hydrogen content and their blue luminosity. These objects are especially important for galactic evolution models, because they appear to be much less evolved galaxies than ours and because they also show obvious signs of recent bursts of star formation.

(ii) From the comparison between their helium and their metal content we can deduce the primordial abundance in helium. This is one of the basic parameters to select among the many possible cosmological models describing the early phases of the Universe. Moreover and within the canonical Big Bang model it could provide some insight on a few characteristics of the physics of elementary particles, such as the number of different classes of not yet observed leptons.

2. The Morphology of the Blue Compact Galaxies

Two recent kinds of surveys have been performed. One of spectroscopic nature by Kunth and Sargent (1979: *Astronomy and Astrophysics Suppl.*, **36**, 259; 1980: ESO preprint no. 99) and a photographic one by Barbieri et al. (1979: *Astronomy and Astrophysics Suppl.*, **37**, 541).

These objects, which do not seem to belong to a specific category of the Hubble classification (there are a few elliptical-like galaxies which can be considered as blue compact objects), are mainly characterized by their relatively small size – the size of the emitting region is only a fraction of a kpc. They show strong emission lines (see e.g. a typical spectrum of Tol 116 in Fig. 1) and have quite a faint absolute visual magnitude

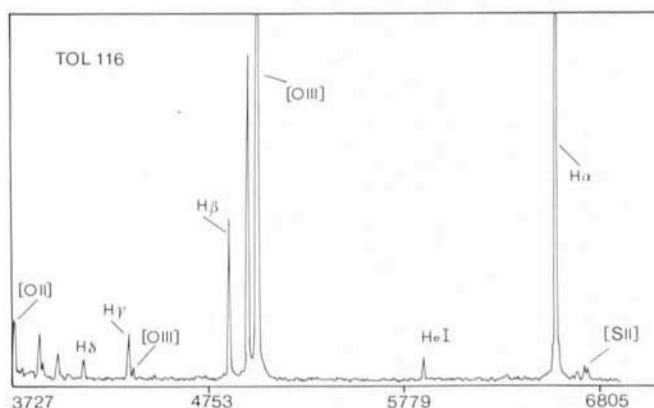


Fig. 1: This is a spectrum of Tololo 116 taken by J. Audouze and M. Dennefeld at La Silla with the IDS at the Cassegrain focus of the 3.6 m telescope.

($M_V \geq -17$). Their colour indices U-B and B-V range respectively between -0.4 and -0.75 and 0.4 and 0.0 .

The total mass of these objects can be estimated by the classical (but not very accurate) method of the velocity dispersions. For instance in the case of I Zw 129 and II Zw 70, O'Connell and Kraft (1972: *Astrophysical Journal*, **175**, 335) found quite low velocity dispersions (25–30 km/s), no evidence for unusual gas motion and deduced masses of the order of a few $10^9 M_\odot$.

These galaxies have been thoroughly analysed in 21 cm (see for instance Balkowski et al. 1978: *Astronomy and Astrophysics*, **69**, 263). Their gas content compared to their total mass can be as high as 0.22 in the case of II Zw 70. They really appear to be among the most gas rich galaxies. A careful mapping of II Zw 70–71 revealed that these two galaxies form an interacting system. By combining infrared with radio observations Jaffe et al. (1978: *Astrophysical Journal*, **224**, 808) seem to propose that II Zw 40 has a gas/dust ratio similar to that of our galaxy. This type of conclusion is a bit surprising when one considers the apparent low metallicity of these objects.

To summarize, although their optical morphology is fairly heterogeneous, a large fraction of these galaxies are among the lightest, the most irregular and bluest galaxies. Their irregularity and small mass suggest that they should be *a priori* less affected by dynamical effects, such as spiral structure, and should accrete very little extragalactic material. We also point out that up to now there is no clear evidence of an underlying stellar old population which would have a direct implication on the nature of these objects (see Section 4.2).

3. The Composition of the Blue Compact Galaxies

The analyses of the composition of these rather unevolved galaxies are performed in the same way as those of the HII regions. We have observed such objects ourselves, like Mark 750, CPG 217 and Tololo 116, by using the ESO 3.6 m telescope on La Silla, equipped with the Boller and Chivens spectrograph and the Image Dissector Scanner. From the [OIII] lines one can deduce the temperature of the emitting gas, which is about 10^4 K, while the electron density, as deduced from the [SII] lines, amounts to a few hundred electrons cm^{-3} . The ionized mass is of the order of $10^6 M_\odot$.

Since the problem of line transfer is not crucial, the derivation of cosmic abundances from observed intensities is straightforward. The major problem in giving the final abundances is the correction made to account for unseen ionization stages.

From various authors one may stress that the metal content of these objects is strikingly deficient as compared to the Standard Abundances.

In the case of I Zw 18 the O/H deficiency is as high as 37. The less deficient objects show underabundances by factors of about 3. The same trend is observed for Ne, N and S and also the helium content, which make these objects suitable for a discussion of the primordial helium.

Notice that the abundances of Magellanic type irregular galaxies (LMC, SMC, NGC, 6822) are within the range of abundances found for these compact galaxies, although never so extreme.

4. Astrophysical Implications

The implications of these observations concern:

- (i) the evolution of these objects. In this respect one would like to know if they underwent bursts of stellar formation, when these bursts occurred and what triggered them.
- (ii) the primordial helium content.

4.1. Chemical Evolution of the Blue Compact Galaxies

Because of the high gaseous content and the low metallicities of blue compact galaxies, it is important to analyse the evolution of these objects, which is fairly easily accounted for, theoretically.

As noted by Audouze and Tinsley (1976: *Annual Review of Astronomy and Astrophysics*, **14**, 43), when the gas content is still high, the so-called Instant Recycling Approximation holds, i.e. one can neglect the lifetime of the stars with respect to the evolution time scale of the system, the relations describing the evolution of the gas density and the metallicity can be solved algebraically. In particular, one can define the yield of metal production, i.e. the amount of metal produced per unit of mass locked into stars.

In the so-called "simple models" where this approximation is made, the relation between the metallicity Z , the gas content and the yield p is $Z = p \ln(M_{\text{tot}}/M_{\text{gas}})$.

This relation has been well verified in the case of the sample studied by Lequeux et al. (1979: *Astronomy and Astrophysics*, **80**, 155). With a linear least square fit on their data they find:

$$Z = (-0.03 \pm 0.16) 10^{-2} + (3.9 \pm 0.10) 10^{-3} \ln \frac{M_{\text{tot}}}{M_{\text{gas}}}$$

which means that the yield in blue compact galaxies is $\sim 10^{-3}$. This implies that the primordial metallicity for these galaxies might have been zero and that the value of the yield deduced from this relation is therefore quite consistent with the values deduced by Pagel (1978: *Monthly Notices of the Royal Astronomical Society*, **183**, 18) and Pagel and Patchett (1975: *M. N. R. A. S.*, **172**, 13) for the solar neighbourhood ($p = 5 \pm 1 \cdot 10^{-3}$). This yield can only be reproduced in models of chemical evolution if one takes into account important stellar mass loss effects (Chiosi and Caimmi, 1979: *Astronomy and Astrophysics*, **80**, 234): theoretical models lead to yields as high as $1.3 \cdot 10^{-2}$ without mass loss and $2 \cdot 10^{-4}$ to 10^{-3} with mass losses. The mass loss processes, which might be related to the blue colour of these objects and to their high ionization rates, are necessary to account for their evolution.

One can notice also that there may be a relation between the total mass of the galaxies and their metallicity. According to Lequeux et al.: $\text{Log } M_{\text{Tot}} = 8.18 + 230 Z$ where M_{Tot} is expressed in solar masses. We believe that this relation is just an indicative trend, the lower limit of $10^6 M_\odot$ should be considered with much caution.

Finally, the Ne/O ratio is normal, which means that Ne is as primary as O. By contrast, N/O is about twice as small in these galaxies as it is for Orion or the Sun. The scatter of the observed N/O ratios, however, clearly indicates that N is neither purely primary nor purely secondary; this conclusion would agree with the findings of Alloin et al. (1979: *Astronomy and Astrophysics*, **78**, 200) from HII regions observed in spirals.

4.2. Stellar Bursts in Blue Compact Galaxies

The blue colour of these objects is due to a presently intense rate of star formation. The concept of burst seems to apply very well to this class of galaxies, since their low metallicity indicates that the present rate of star formation exceeds much the average rate in the past. The basic question (which may be a pure semantic one) is to know whether these galaxies are young and experience their first burst, or if these objects are old, have already formed stars and are just suffering a new burst.

This question has not yet received convincing answers. Searle and Sargent (1972: *Astrophysical Journal*, **173**, 25), on statistical grounds, argued that these galaxies must be old.

However, Lequeux and Viallefond (1981: *Astronomy and Astrophysics*, in press) have been able to investigate this problem in the case of I Zw 18. For this object, they compare the luminosity due to ionizing Lyman continuum photons, the far UV flux around 1700Å, which is mainly due to the B0,B5 stars, the blue luminosity and the abundance of oxygen. By using current models of chemical evolution of galaxies, such as those which describe the evolution of their luminosity, they show that the luminosity in the Lyman continuum and the luminosity in the far UV evolve differently with time. The Lyman continuum luminosity depends on more massive stars than the far UV and the visible luminosity. From the observed properties of I Zw 18 they argue that a recent burst of duration 4-6 10^6 years might be responsible for the major part of the observed oxygen. They would conclude that I Zw 18, which appears to be formed of about six debris interacting gravitationally, is just starting its first burst of star formation.

Tentative Time-table of Council Sessions and Committee Meetings in 1981

May 4	Committee of Council
May 7-8	Finance Committee
May 7	Scientific Technical Committee
May 8	Users Committee
May 21-22	Observing Programmes Committee
June 4	Council, Stockholm
November 10	Scientific Technical Committee
November 11-12	Finance Committee
November 13	Committee of Council
Nov. 30-Dec. 1-2	Observing Programmes Committee
December 3-4	Council

All meetings will take place at ESO in Garching, unless stated otherwise.

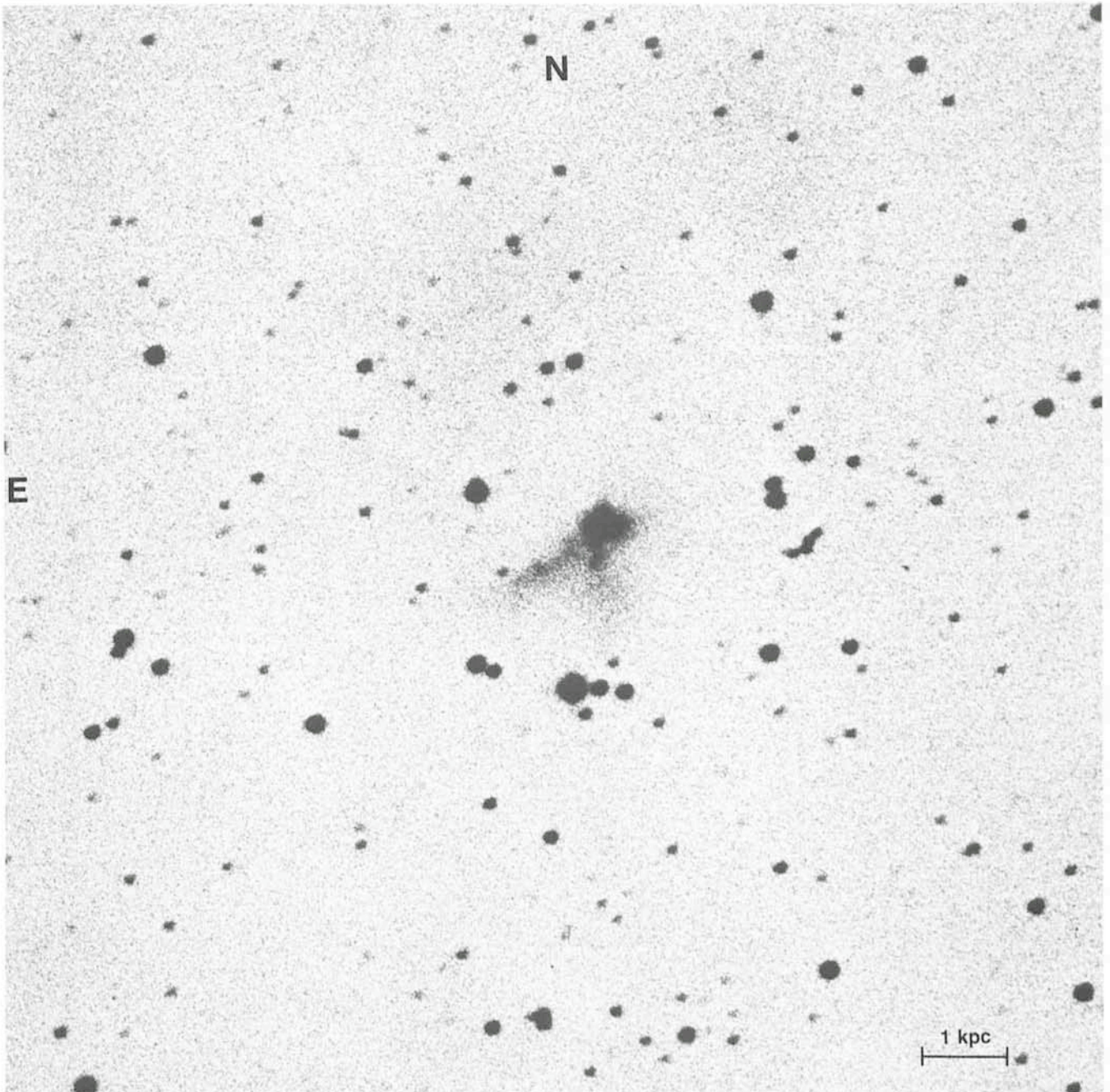


Fig. 2: This is a blue picture of I Zw 40 taken at the prime focus of the 5 m telescope at Palomar and lent to D. Kunth by W. L. W. Sargent. North-East is at the top left corner. The scale shows the distance in kiloparsec.

This conclusion may apply only to I Zw 18 among the known compact galaxies. Lequeux and Viallefond would propose that other galaxies, such as II Zw 70–71, which are more complex, rotating, and which have had time to become relaxed systems, are older than I Zw 18.

4.3. The Primordial Helium Abundance

Let us denote by Y the fractional helium abundance by mass. A comparison between the helium and the metal content implies that the corresponding galactic enrichments ΔY and ΔZ are proportional: $\Delta Y = \alpha \Delta Z$ with $\alpha \approx 3$. Again such a high value for α can only be reproduced in models of chemical evolution involving important stellar mass loss. Without mass loss, the α coefficient would only be at most 0.5 to 0.1. This can be easily understood if one recalls that helium can be reproduced by low-mass stars, while in massive stars the metal enrichment increases more than the helium enrichment.

Recent studies have been devoted to the determination of the primordial helium abundance by extrapolating Y to $Z = 0$. Lequeux et al. (1979: *Astronomy and Astrophysics*, **80**, 155) and, more recently, Kunth and Sargent (1981: in preparation), on a wider sample of blue compact galaxies, have discussed this relation (Y, Z), out of which the "primordial" value seems to converge to about $Y_p = 0.235 \pm 0.010$ with the value quoted above, and by adopting the canonical¹ Big Bang theory to account for the early phases of the Universe, one can deduce an upper limit for the present density of the Universe $\rho \leq 3\text{--}5 \cdot 10^{-31} \text{ g cm}^{-2}$ (see e.g. Yang et al. 1979: *Astrophysical Journal*, **227**, 697).

Therefore, the Universe is expanding for ever (it is open!); the primordial nucleosynthesis is able to account for the observed abundances of deuterium. Moreover, it provides a quite strict limit on the number of possible different families of leptons, which should be ≤ 3 . If the discovery of the tau lepton is confirmed, one should not find any new type of leptons unless the canonical Big Bang models do not apply. From such conclusions, the observations of the blue compact galaxies are of prime importance in cosmology.

5. Conclusion

Significant progress has been made on this class of quite unevolved galaxies.

(i) their primordial content of helium now seems to be well established $Y = 0.233$ and is consistent with an open Universe, a canonical Big Bang model and no unknown type of leptons.

(ii) The helium over metal enrichment is about 3 and seems to indicate that the stellar mass loss plays an important role in fixing this ratio at this value.

(iii) The blue compact galaxies are quite unevolved: one galaxy, I Zw 18, has an oxygen abundance about 40 times lower than the solar value. They are well described by the simple models with instant recycling approximation. This means that their primordial metallicity might have been equal to zero. The value of the yield, deduced from the comparison of the metallicity with the gas content, implies that stellar mass losses should operate. Moreover, there is a correlation between the metallicity and the total mass of these galaxies, for which nitrogen appears to be partially secondary.

(iv) These objects have very different morphological aspects although they have rather low masses, high intrinsic luminosities, conspicuous hot HII regions and blue colours. Some of them are isolated, while a few others, like II Zw 70, belong to interactive systems. One of the most intriguing object is I Zw 18, which seems to be made of several interacting debris which have just experienced a very recent burst of star formation. The differences between some of the blue compact galaxies might come from the time when the bursts of star formation occurred.

The advent of forthcoming UV missions, like the space telescope or the post IUE projects, will obviously reveal more characteristics of these very important galaxies: their actual nature and why their rate of star formation is sudden rather than continuous. It would allow better determinations of mass loss effects, and measurements of the composition in carbon. As it has been seen for I Zw 18, the far UV luminosity provides some information on the occurrence of the stellar bursts. Moreover, if (as it is expected in UV projects like Magellan) the 900–1100 Å wavelength is observable, a direct measurement of the deuterium abundance in such unevolved objects would be of utmost interest for cosmological models.

PERSONNEL MOVEMENTS

STAFF

ARRIVALS

Europe

VÖLK, Elisabeth, D, Secretary, 1.11.1980
GUSTAFSSON, Karl, S, Analyst/Programmer, 1.1.1981
HESS, Guy, F, Designer/Draughtsman, 1.1.1981
POMAROLI, Edouard, F, Electro-mechanician, 1.1.1981

DEPARTURES

Europe

ANDERSSON, Sölve, S, Electronics Technician, 31.12.1980

Chile

VOGT, Nikolaus, D, Astronomer, 30.11.1980

ASSOCIATES

ARRIVALS

Chile

NISSEN, Poul, DK, 1.2–31.7.1981

FELLOWS

ARRIVALS

Europe

BAADE, Dietrich, D, 1.2.1981
BENVENUTI, Piero, I, 1.2.1981
KRUSZEWSKI, Andrzej, Poland, 1.2.1981

DEPARTURES

Europe

MELNICK, Jorge, Chile, 28.2.1981

COOPERANTS

ARRIVALS

Chile

ANGEBULT, Louis, F, Coopérant, 29.10.1980

¹ In such models one assumes that:

- (i) the early Universe was homogeneous and isotropic,
- (ii) there was no significant amount of antimatter,
- (iii) General Relativity accounts well for the gravitational interactions,
- (iv) the leptons are non degenerated,
- (v) there were no unknown elementary particles, and
- (vi) the early phases of the Universe were dense and hot ($T > 10^{11} \text{ K}$)

Physical Studies of Asteroids – an Observing Programme at ESO

Claes-Ingvar Lagerkvist, Astronomical Observatory, Uppsala

Introduction

The majority of the asteroids are small and tiny bodies orbiting the sun between Mars and Jupiter. One can estimate the total number of asteroids with diameters greater than 1 km to be more than 700,000. Compared to the major planets, the thermal and geological evolution of the asteroids has been modest. Observing asteroids gives us thus not only clues to the origin and evolution of the asteroids, but also to that of the planetary system.

This article attempts to give a short description of the programme "Physical Studies of Asteroids" for which the major part of the observations is conducted at ESO, La Silla. One part of the programme deals with detailed studies of rather bright asteroids, aiming at a better understanding of rotational properties, shapes, compositional types and other physical parameters essential for studies of asteroids. Correlations between rotation period and size, period and compositional type, shape and size, and properties of family asteroids, are some of the problems studied with the aid of photoelectric UVB photometry. Another part of the programme deals with the properties of the very small asteroids, which have sizes of only a few kilometres. How have these been formed? Are they collisional products or do they more resemble the original planetesimals? What is their history of evolution? The ESO Schmidt telescope has been used to study these questions.

Studies of Bright Asteroids

Figure 1 presents a lightcurve of the asteroid 250 Bettina, obtained during September 1980 with the ESO 50 cm telescope. If we assume that the lightcurve shows two maxima and

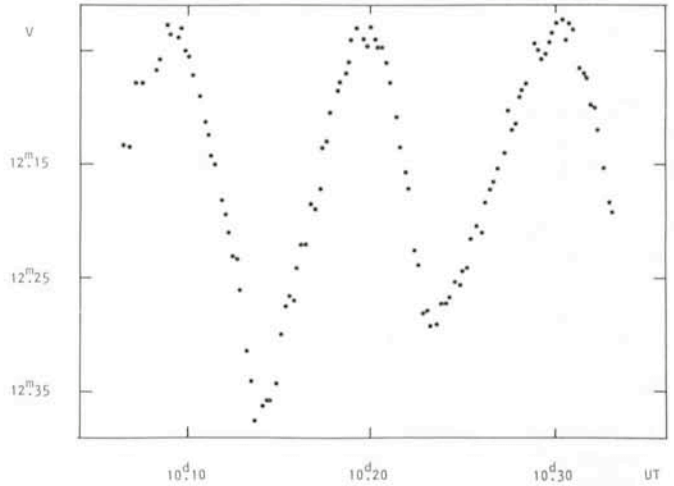


Fig. 1: Photoelectric lightcurve of the asteroid 250 Bettina observed with the ESO 50 cm telescope on September 10, 1980. The observed V magnitude is plotted versus universal time. 250 Bettina has a rotation period of $5^h.1$.

two minima per rotation cycle (the normal triaxial model that seems to work quite well for more than 90 % of the asteroids), thus supposing that the change of brightness depends on the shape of the asteroid rather than on variations of the albedo over the surface, we get for 250 Bettina a period of $5^h.1$. Only one asteroid, Vesta, has a lightcurve indicating that the change in brightness depends on variations of the albedo over the surface of the asteroid. Some asteroids have lightcurves showing three maxima and minima per rotation cycle and they

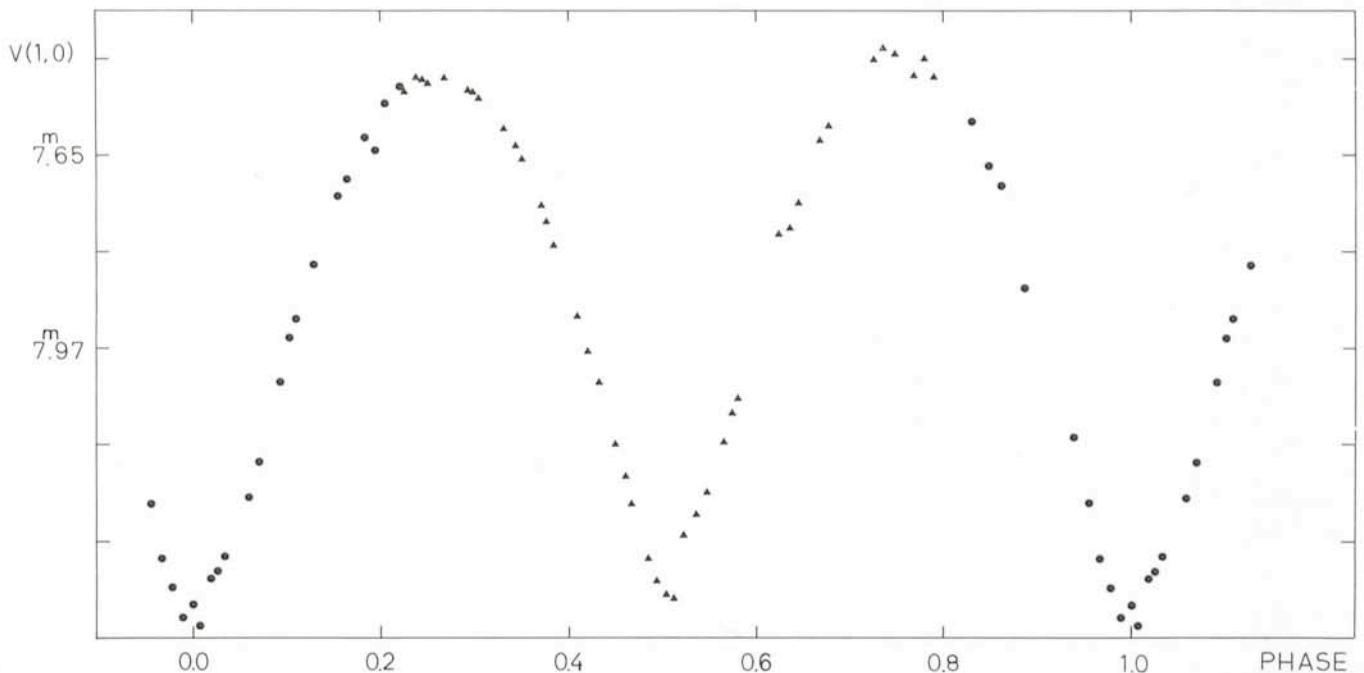


Fig. 2: composite lightcurve of 63 Ausonia observed at ESO during two nights in March 1980. The absolute magnitude ($V[1,0] = V_{obs} - 5 \log [r \cdot \Delta] - 0^m.035 \cdot \text{phase angle}$) is plotted versus phase. The amplitude of $0^m.95$ is remarkably large for an asteroid with a diameter of nearly 100 kilometres. 63 Ausonia has a period of $9^h.3$.

are thus of a somewhat more complicated shape than the normal triaxial model.

Figure 2 displays a composite lightcurve of 63 Ausonia, observed in March 1980 with the ESO 50 cm telescope. Ausonia is nearly 100 km in diameter and the lightcurve amplitude, 0^m.95, is remarkably large for an asteroid of this size. No other main-belt asteroid this big has such an irregular shape.

UBV observations of asteroids provide us not only with information about the rotation periods and shapes, but give also information about the composition of the material on the asteroids' surfaces. Most asteroids can be divided into a few distinct compositional types from their UBV colours. The most common types are: *C* (carbonaceous chondrites), *S* (silicaceous) and *M* (metallic). Of the asteroids greater than 50 km in diameter, 76% are of type *C*, 16% of type *S*, 5% of type *M*. From the colour indices $B-V=0^m.70$ and $U-B=0^m.27$ we can classify 250 Bettina to be of a compositional type close to *M*. Because of the small number of *M* asteroids, only a few have been observed so far, but there are indications that the asteroids of type *M* have a faster spin than the other asteroids. The reason for this may be that they have a greater density. Another asteroid of this type, also observed at ESO in September 1980, 201 Penelope, has a period of about 4 hours.

During four observing runs at ESO a total of 15 asteroids have so far been observed long enough to make it possible to determine their rotation periods. Table 1 summarizes very briefly some of the results obtained during the first three observing runs. During August/September 1980 about 20 lightcurves were observed of the asteroids 33, 101, 201, 250, 386 and 432.

The ESO 50 cm telescope has proved to be very efficient for this type of observations. The accurate setting of the telescope makes finding charts unnecessary, accurate coordinates taken from the yearly volume of the *Ephemerides of Minor Planets* is

Table 1. Physical data for some of the observed asteroids

Asteroid	Period	Amplitude	B-V	U-B	Type
63	0 ^m .3873	0 ^m .95	0 ^m .92	0 ^m .53	S
64	0 ^m .365	> 0 ^m .44	0 ^m .74	0 ^m .28	CME
85	0 ^m .2864	0 ^m .16	0 ^m .67	0 ^m .30	C
95*	0 ^m .3620	0 ^m .25	—	—	—
133*	0 ^m .5293	0 ^m .25	0 ^m .90	0 ^m .51	S
135	0 ^m .429	0 ^m .17	0 ^m .70	0 ^m .28	CME
218*	0 ^m .268	0 ^m .22	0 ^m .86	0 ^m .44	S
485*	0 ^m .7331	0 ^m .12	0 ^m .85	0 ^m .43	S
683*	0 ^m .1801	0 ^m .12	0 ^m .69	0 ^m .31	C
792*	0 ^m .382	0 ^m .62	0 ^m .71	0 ^m .21	M

* Observer M. Carlsson

enough for having the asteroid more or less in the diaphragm after setting the telescope. Since the telescope is computer-controlled, it is possible to observe quite fast; during September 1980 it was thus possible to observe the asteroids 33 Polyhymnia, 101 Helena and 386 Siegena more or less simultaneously during the same night. 101 Helena seems to have a period close to 24^h but the other two rotate faster.

Studies of Small Unnumbered Asteroids

Most of the plate material was collected with the Schmidt telescope at ESO during 5 nights in 1978–1980. Many plates of the same field in the ecliptic, taken during the same night, make it possible to obtain photographic lightcurves of a large number of small unnumbered asteroids. Kodak plates of type 098–04, combined with the Schott filter GG 495, give a limiting magnitude of $V \sim 18^m$ (exposure time 5–6 minutes). The unnumbered asteroids are found on a plate with long exposure time, thus

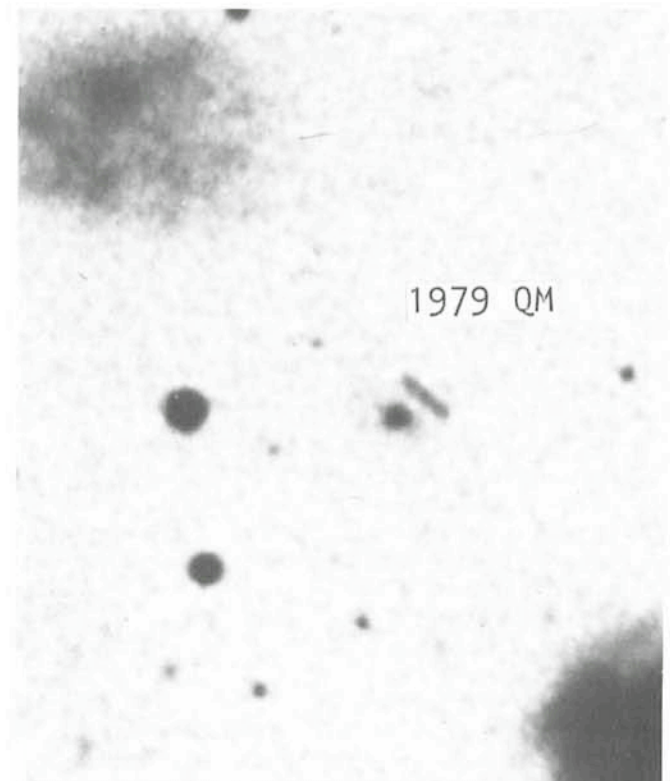


Fig. 3: Two out of several hundreds of asteroids found during the work. The asteroid 1979 QM is probably an Amor asteroid. The large diffuse spots are just ink dots marking the asteroids' trails.

making it quite easy to pick out the trails of the asteroids among the round images of the stars. This has given for each of the observed fields almost 150 newly discovered asteroids. Figure 3 is a copy of a part of a plate taken during August 1979. The figure shows the trail of an ordinary main-belt asteroid, 1979 QU2, and that of a faster-moving object, probably an Amor asteroid (an asteroid with perihelion well inside the orbit of Mars).

Additional plates are taken for positions in order to derive orbital elements, and thus distances, and, from that, estimates of the diameters of the asteroids. The positions on some of the plates from 1979 were measured with the ESO Optronic machine, giving nearly 800 positions of some 140 newly discovered asteroids. Since this part of the programme still is in a preliminary phase, it is too early to draw any conclusions about the physical nature of the small asteroids.

Mapping the Southern Sky with the ESO 1 m Schmidt Telescope

H.-E. Schuster, ESO

To any astronomer, professional or amateur, the Palomar Observatory Sky Survey (shortly POSS) is a well-known and useful tool. The whole northern sky is photographed and prints from these photographs are available in the libraries of nearly all important observatories and astronomical institutes in the world.

Such a collection of photographs represents a sort of inventory of the universe, at least of the part accessible with our present instrumentation. In a simple way, this photographic inventory serves just to see what we have in the sky. What stars, clusters, nebulae, galaxies are there? Later, having done a selection, astronomers may concentrate on single objects or classes of objects for a deeper detailed investigation.

It is not necessary to explain here at long the importance and usefulness of the Palomar Sky Survey. In a certain sense it has become a "classic" already and has set a landmark and a high level in the field of sky mapping. Its only disadvantage, if one may say so, is the fact that it is limited to the northern hemisphere.

So, since the end of the fifties when the POSS had been finished and distributed to the astronomers, there has been the wish and the need to have a similar atlas of the southern sky.

One large obstacle to such an atlas was the fact that there was no adequate instrument available in the south for making the survey.

The instrument best fitted for such a photographic survey is a wide-angle camera with the following three important specifications:

- (1) as already mentioned, it should have a wide field, otherwise it would be necessary take thousands of plates to cover a certain range of the sky, instead of only a few hundred;
- (2) it should be powerful in "light-catching", in order to reach faint objects, or, roughly spoken, it should look into the sky as deep as possible;
- (3) and the plate scale should be reasonably large as for extended objects, galaxies for instance, a fair resolution would help the user of the survey to try a first morphological classification of the objects.

The instrument of best choice is then, in consequence, a Schmidt camera.

There have been Schmidt cameras in operation in the south since long, but of smaller size and not as powerful as the Palomar Schmidt telescope. Once the northern atlas had been completed, one wished of course not only just a continuation to the south but a continuation which would be compatible. That means: the same field size, or nearly the same, the same

limiting magnitude, or better if possible, and the same scaling in order to have comparable overlapping fields.

During the seventies, two large Schmidt telescopes came into operation; they had exactly the same scale as the Palomar Schmidt (1 mm = ~ 67 arcseconds) and fulfilled also the specifications of power and field size. These are the United Kingdom Schmidt telescope, based in Australia, and the ESO 1 m Schmidt telescope on La Silla. Both telescopes are now engaged in producing maps of the southern sky similar to the great example the Palomar Survey has set.

The laborious task has been distributed in such a way that both telescopes are busy with maps of different colours. ESO has taken the part of producing an atlas in the RED range, which is being realized on the fine grain KODAK IIIa-F emulsion behind a filter RG 630. In this way, a band-pass is defined from

Second ESO/ESA Workshop on the Use of the Space Telescope and Coordinated Ground-based Research

ESO, Garching, 18–19 February 1981

Optical Jets in Galaxies

List of Topics

- Introduction: Jets and other evidence for outflow in active galaxies
- The ST – important parameters for planning observations
- Imaging observations of optical emission from jets
- Spectroscopic evidence for collimated outflow in active galaxies
- The M87 jet
- Centaurus A
- QSO jet: 3C 273 and other QSO jets
- Coma A
- Radio emission from jets
- X-ray emission from jets
- Relevant theoretical aspects
- Discussion
- Concluding remarks

Organizers: F. Macchetto, ESTEC — G. Miley, Leiden — M. Tarenghi, ESO.

about 6300 to 6900 Å with the famous H-alpha line included. The exposure time for each plate is 2 hours, which is quite a task for a large-field camera aiming at the ideal condition to have good images all over the field of 5.5 x 5.5 degrees. The KODAK IIIa-F emulsion is a fine-grain emulsion, which results in high resolution, but the plates have to be pretreated before being used in the camera. This rather complicated and somewhat "tricky" process of sensibilization has to be applied; otherwise the response of the emulsion to light would be very low.

As a standard, at present, the plates are heated under 65° C in a gas flow of 2 liters per minute, in the following way: for 30 minutes in pure nitrogen gas and then another 2 hours in a mixture of 96% nitrogen and 4% hydrogen. This method is liable to variations depending on the original quality of the emulsion which varies with age and also intrinsically between

factory delivery. So nearly permanent tests are necessary to have the emulsion under control.

The ESO RED atlas is under work at present, and about 5 to 6 years will be necessary to complete the 606 fields covering the sky from declination -17°5 down to the southern celestial pole.

It is a rather time consuming and sometimes difficult work to produce the necessary 606 master plates which are copied later for distribution.

Many parameters have to be obeyed carefully in order to get a good acceptable plate worth to be copied. Sensibilization may fail, intrinsic emulsion faults, i.e., scratches or holes in the emulsion, unproper development, breakage of the plate, guiding errors during the exposure are only some of the problems which may occur and disqualify a plate to be an original for copying.

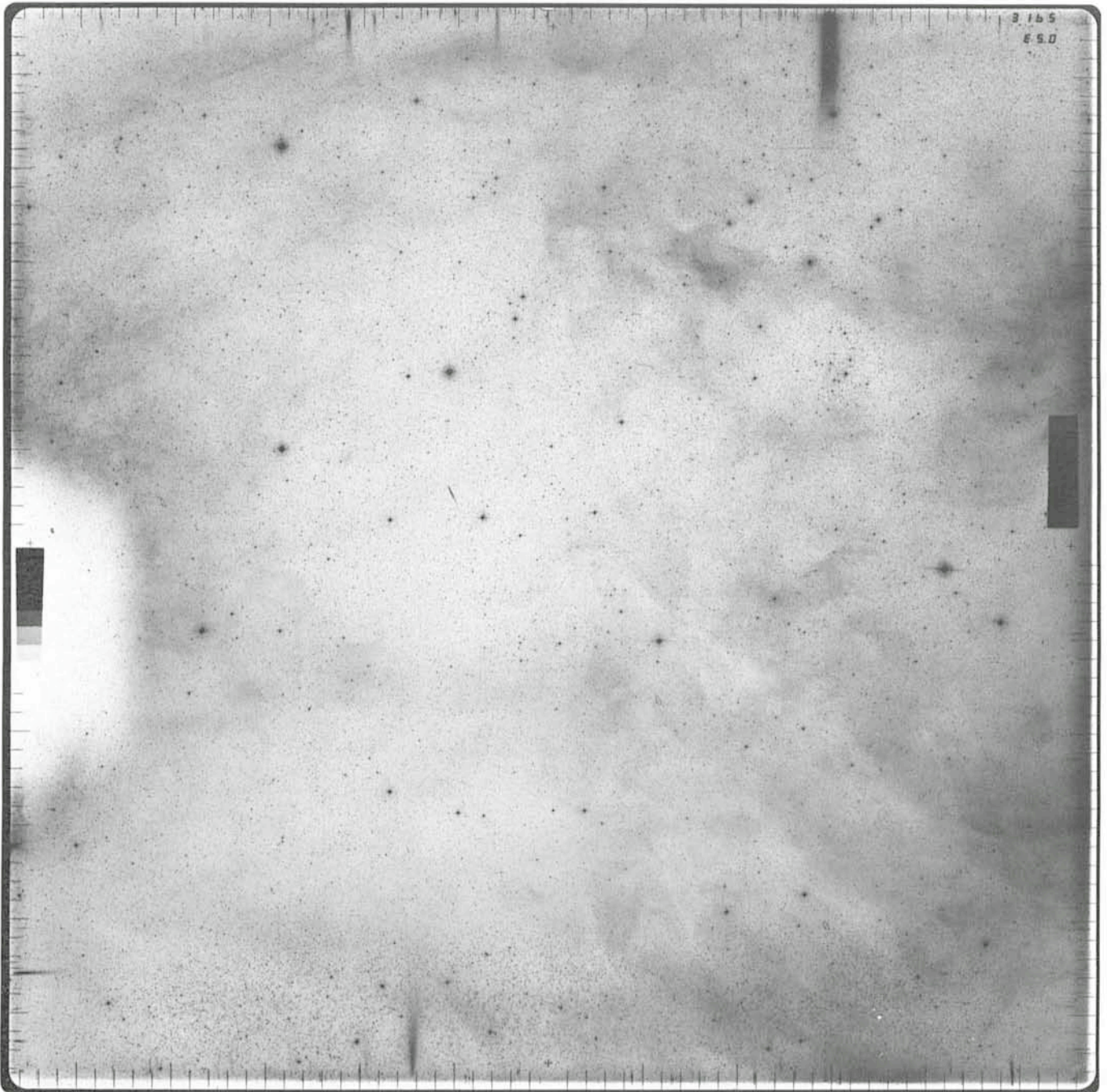


Fig. 1: Field No. 209 of the RED atlas is one of the first already distributed fields.

In addition, there are what we may call problems put by nature: moontime, clouds and bad seeing, which do not permit us to take atlas plates of high standards and cause delay in production.

To get a dozen good plates is nothing worth to be mentioned, but to have 606 plates of equally good quality in a reasonably limited time is something which can be fully appreciated only by somebody who has been busy himself in atlas and mapping projects, even if this may appear a little bit arrogant. And this refers only to the production of the master plates; another and certainly also troublesome task is the copying process, which is done in Europe – that is to obtain from one good original the necessary 20 or 50 or 100 equally good copies.

Fortunately, ESO could achieve a lot of valuable experience in atlas work before starting the above-mentioned RED atlas.

Experience which resulted in improvements of the telescope and skills and "know-how" concerning plate handling and copying processes.

ESO had been busy for some years already in producing a BLUE atlas of the southern sky. This so-called Quick Blue Survey or QBS was completed about one and a half year ago and has been distributed to many observatories in ESO countries and others.

The same 606 fields are covered as now for the RED atlas; the emulsion of the plates used was KODAK IIa-O behind a filter GG385 giving a band-pass from about 3850 to 5000Å; the exposure time was one hour, and a limiting magnitude of 20.5 to 21 is reached. We hope to get deeper with the aforementioned RED atlas, possibly to the 22nd magnitude. To get the 606 good master plates for the finished BLUE atlas, altogether 1039 plates had to be taken, which leads to a ratio of 58 %



Fig. 2: Infrared plate (IV N + RG 715) of the Large Magellanic Cloud.

accepted plates to 42% rejected ones. It is interesting to note that this ratio is nearly exactly the same as the one of the Palomar group with the northern atlas.

Rejected plates are not completely useless; many of them have only a scratch or an unaesthetic patch, or a broken corner — details which do not allow them to be copied, but they are still useful and stored together with the master plates in the ESO files in the Garching archives.

The ESO Quick Blue Survey is now in full use and a direct follow-up work is also nearly finished. In collaboration with Uppsala Observatory, ESO has scanned the 606 southern sky fields, and any object larger than 1 mm (or about 67 arcsecs) is compiled in a catalogue, with the coordinates and a preliminary description. This catalogue, which contains several thousand objects, and the sky surveys done in Chile and Australia are the basis for future photometric and spectrographic programmes with the large telescopes now in operation in the south.

As said above, moontime does not permit us to take BLUE or

RED atlas plates, the background would get too high. There exists, however, a combination of emulsion and filter which makes it possible to work even during full moon and to reach a colour band-pass which has become more and more of interest for astronomers. Using a KODAK IV-N emulsion with a filter RG715 the so-called near infrared is covered. The IV-N emulsion needs a careful wet sensibilization in a solution of silvernitrate, and then an immediate drying before use in the telescope. ESO has in its files in Garching a selected atlas along the band of the southern Milky Way. This IR atlas is not meant for distribution but available for use in Garching. On the other extreme of the spectrum, the ultraviolet has called more and more the attention of astronomers. Sporadically, there are informal talks about an atlas in the UV band. The same talks concern the possibility to have an atlas of objective prism spectra of the southern sky or at least of certain selected areas. But for the moment and for some time in the future the ESO RED atlas is the main task of the La Silla Schmidt.

Simultaneous Optical and Satellite Observations Provide New Understanding of a Famous Nova

H. Drechsel, J. Rahe

Remeis-Observatory Bamberg, and NASA-Goddard Space Flight Center, Greenbelt, MD, USA

A. Holm

Computer Sciences Corporation, Silver Spring, MD, 20910, USA

J. Krautter

Landessternwarte-Königstuhl, Heidelberg

Most stars in our Galaxy appear to be stable and shine with essentially the same intensity over millions of years. Novae (and supernovae), on the other hand, suffer suddenly a gigantic explosion. Their brightness increases in only a day or two by more than several 10,000 times, marking them often the brightest objects in the night sky, before they eventually fade in the course of several years to their former relatively insignificant pre-outburst brightness. These stars were called "novae" (which literally means "new stars"), long before it was realized that they are not new at all, but existed already as stars long before their outburst. Nova Aquilae (1918) is actually one of the very few objects which had been known to exist before it turned into a "nova".

Until now, more than 150 "normal" novae have been recorded in our Galaxy, and typically one or more can be observed in a year. Although many novae remain undetected, it is estimated that about 25 appear per year in our Galaxy.

In the outburst, a shell is ejected with typical velocities of about 2000 km/sec. In many cases, the expansion of this envelope could be followed in direct photographs. In the case of nova V 603 Aquilae (see Fig. 1), the envelope showed a radial velocity of about 1700 km/sec; it expanded by about 1" per year.

It is now generally accepted that novae are in fact close binary systems, consisting of a very compact object, which is probably a white dwarf, and a large, cooler late-type secondary that fills its Lagrangian lobe. The hydrogen-rich material lost by the expanding cooler star flows through the inner Lagrangian

point towards the white dwarf, forming a fast rotating ring of material around it.

To obtain a better understanding of a typical old nova, extended optical observations with the ESO 1.5 and 3.6 m telescopes as well as ultraviolet measurements with the IUE satellite were conducted.

Nova Aquilae (1918) was the brightest new star that appeared in the sky since Tycho's and Kepler's supernovae in 1572 and 1604, which reached a maximum brightness of -4^m and -3^m , respectively (Clark and Stephenson, 1977). It shone with a visual magnitude of $-1^m.1$, on June 10, 1918, and was the brightest nova discovered since the invention of the telescope. It is a spectacular example of a "fast" nova that went through a very sharp light maximum and showed a steep brightness decrease which was followed by pronounced post-maximum fluctuations (Payne-Gaposchkin, 1957). The fading nova was soon found to be surrounded by a small nebula (Barnard, 1919) which expanded at a uniform rate (Mustel and Boyarchuk, 1970), and which by now has essentially vanished (Williams, 1980).

The binary character of nova V 603 Aquilae was discovered by Kraft (1964) from an analysis of Palomar coudé spectrograms. The radial velocity curve had a period of $3^h 19^m 5$ and a rather small amplitude of $v. \sin i = 38 \text{ km s}^{-1}$, which indicates a low inclination of the system. Pronounced eclipses of the accretion disk around the white dwarf by the late main sequence star were therefore not expected.

Although, over the years, light fluctuations were reported by a number of authors, up to now, no photometric measurements

1926

1930

1933

1940

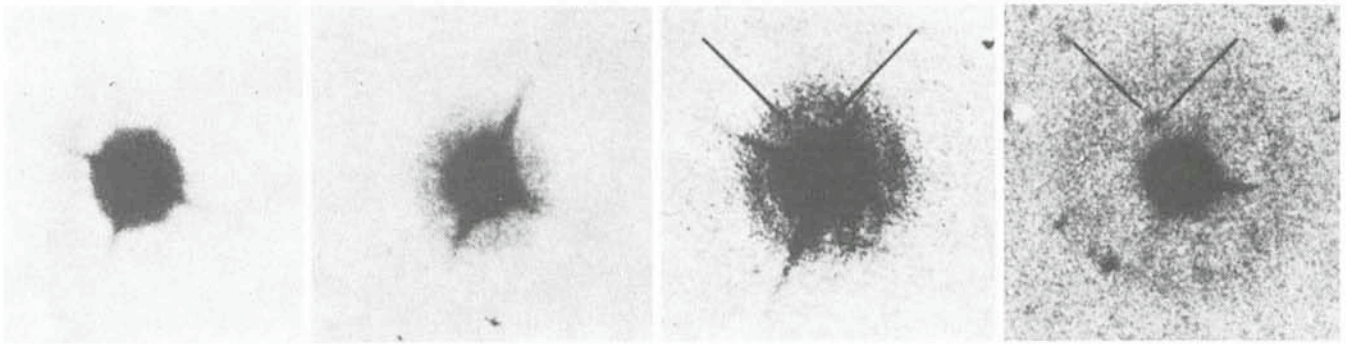


Fig. 1: Photographs of the expanding envelope around the old nova V 603 Aquilae, taken at Mt. Wilson Observatory (from Mustel and Boyarchuk, 1970).

covering time intervals of the order of the binary period have been reported. Now, exactly 62 years after the outburst, on June 10, 1980, the brightness and spectroscopic behaviour of nova Aquilae was monitored for eight hours continuously by the IUE satellite. At practically the same time, as well as earlier and later, the nova was observed with the ESO 1.52 m and 3.6 m telescopes.

Photometric measurements were made with the Fine Error Sensor (FES) onboard the IUE with 5.1 sec integration per observation. The FES is an unfiltered image dissector tube with an S-20 photocathode. In the track mode, the stellar visual magnitude can be derived from the FES count rate for the observed star. These measurements revealed pronounced periodic changes in the lightcurve with an amplitude of about $0^m.3$ and a period of $3^h 18^m.3$ (Rahe et al., 1980). The magnitude during maximum light was about $11^m.7$. A statistical flickering with a typical time scale of one or a few minutes is always superimposed on the lightcurve.

In principal, the light variations could be due to orientation effects. The observed brightness depends on the angle under which the radiating surface is seen. Part of the light comes from

a hot area which arises from the release of kinetic energy of the material transferred from the late star to the accretion disk around the white dwarf. In addition, light can be reflected and re-radiated from those regions of the cool companion which are facing the accretion disk and are thus considerably heated by its radiation and by the white dwarf.

The viewing angle of these surface areas varies periodically with phase and can produce a sinusoidal lightcurve. Such a behaviour was, e.g., observed for the old novae RR Pic 1925 and HR Del 1967. Another, perhaps even more likely explanation is that during the observed minimum phases, the hot area is partially eclipsed by the late companion or the optically thick material of the disk itself. This, however, implies a higher inclination angle than previously assumed.

Strongly correlated with the visual lightcurve are changes in the ultraviolet emission line fluxes of C IV (1548, 1550 Å), Si IV (1393, 1402 Å), and He II (1640 Å) by about a factor of two (Drechsel et al., 1980). The intensity of these lines is highest during maximum light at about phase 0.5 and lowest near orbital phase 0.0. The correlation of their intensity with the orbital motion suggests that they originate in close proximity to

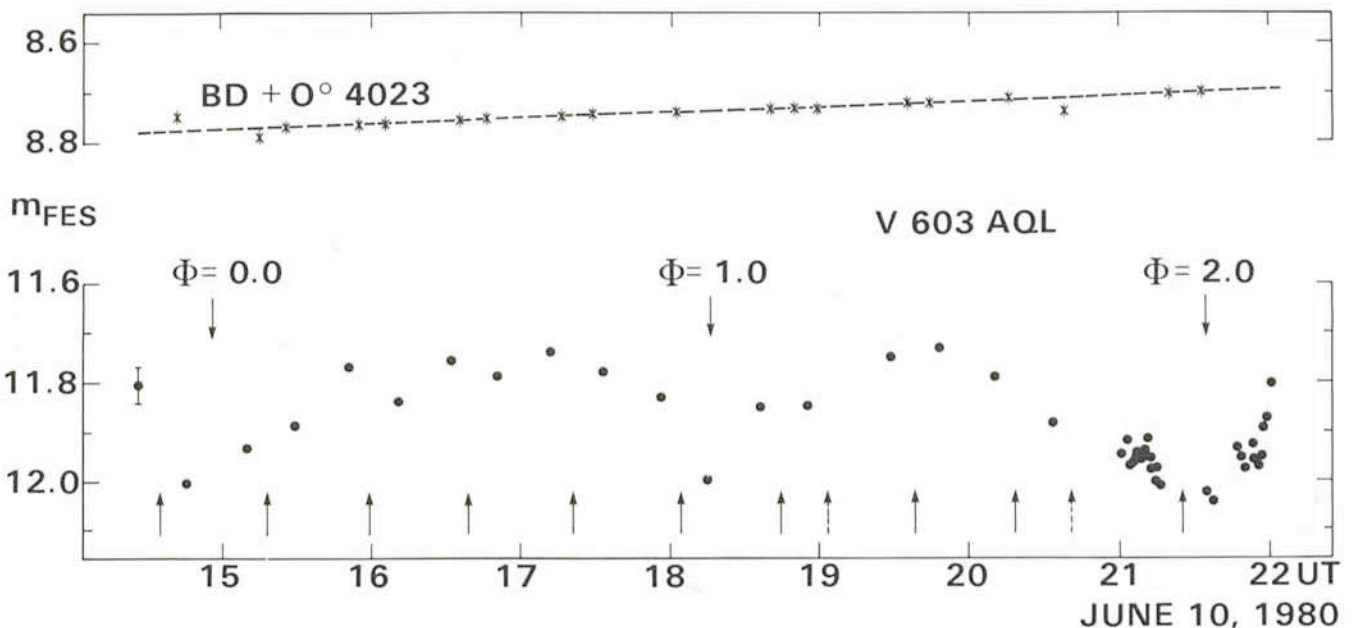


Fig. 2: lightcurve of V 603 Aql as observed with the Fine error Sensor (FES) of IUE, on June 10, 1980, between 14 and 22^h UT. The field star BD + O^o 4023 was used as comparison star. The phases (φ) given correspond to the orbital period of $3^h 18^m.3$ of the close binary system. Arrows at bottom indicate the times of mid-exposure of IUE spectra. These measurements revealed that nova Aquilae is in fact an eclipsing binary.

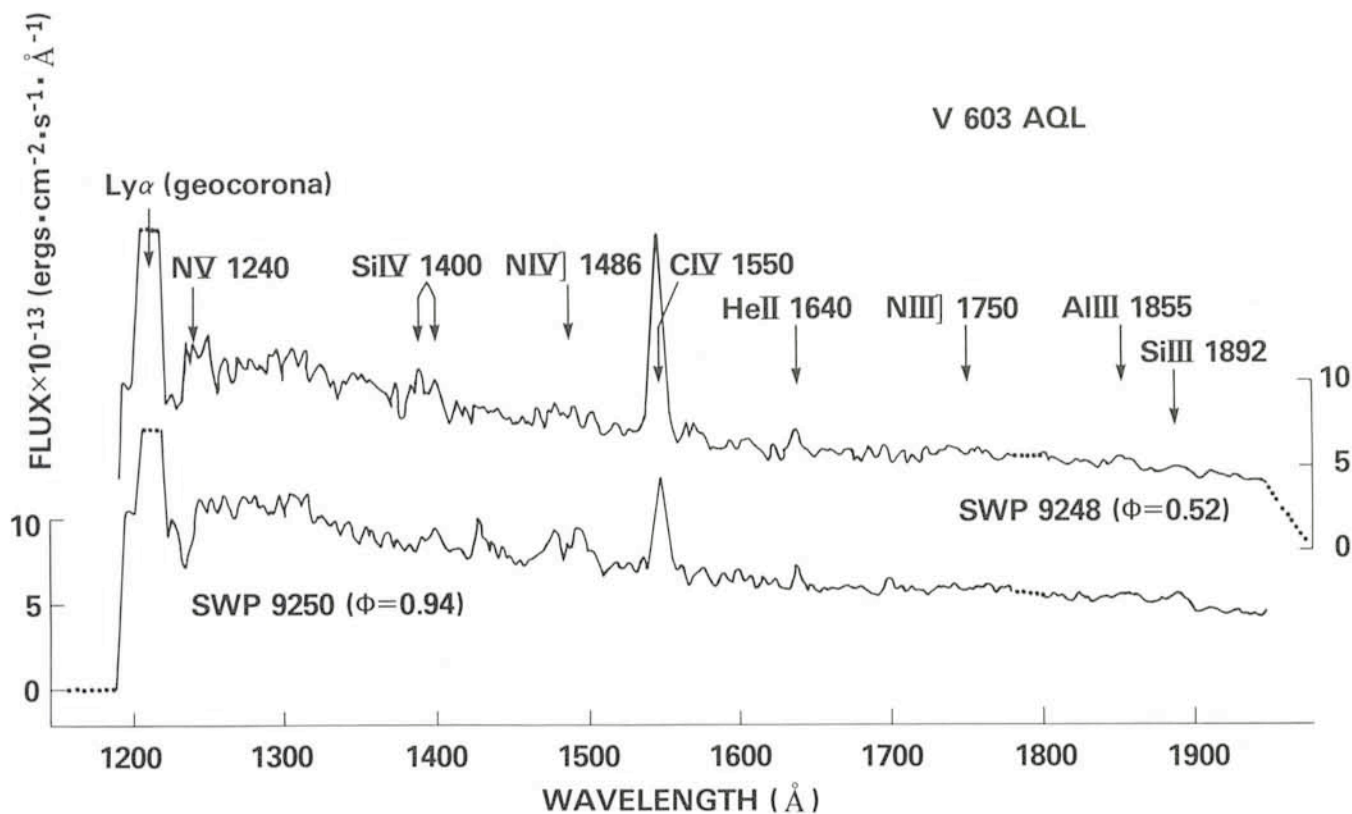


Fig. 3: Two selected IUE short wavelength spectrograms of V 603 Aql obtained at orbital phase 0.52 and during the eclipse at phase 0.94. Pronounced variations of the strengths of C IV (1550), Si IV (1400) and He II (1640) as well as of N IV] (1486) — but in an opposite sense — are clearly noticeable.

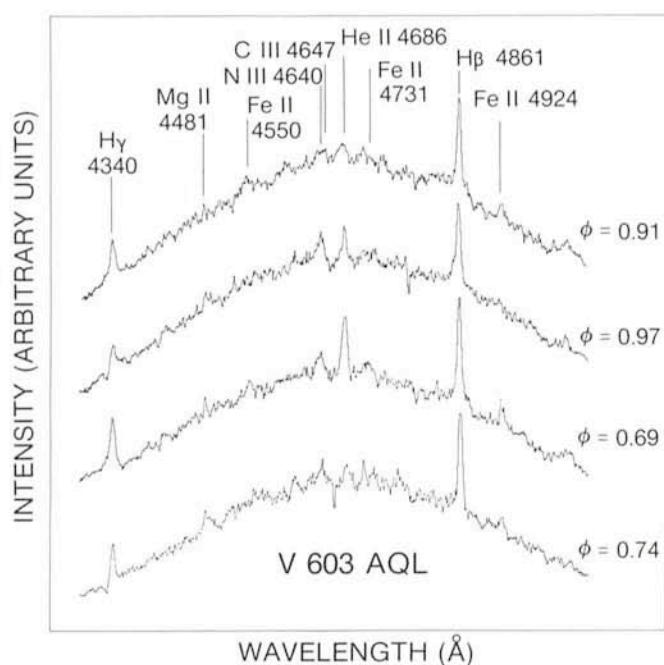


Fig. 4: Optical observations of V 603 Aquilae, obtained in June 1980 with the ESO 3.6 m telescope, equipped with the Boller and Chivens Cassegrain spectrograph and IDS. Dispersion 39 Å/mm, wavelength region 4290-5050 Å. The four spectrograms shown are typical examples of the more than 40 spectrograms obtained continuously during one complete orbital cycle (3^h18^m3) of the close binary. Variations in the line strengths (e.g., He II at 4686 Å) and profiles (e.g., H-gamma at 4340 Å) with the orbital phase ϕ are clearly noticeable.

the two stars. Several semi-forbidden lines can be identified; the most prominent is N IV] (1486 Å). They originate probably in a somewhat extended region of diluted gases, and their intensity is not affected by eclipse effects. The effects of mass transfer from the late main sequence star onto the disk surrounding the white dwarf component should also be noticeable in X-ray observations of this old nova.

More than 40 spectrograms were obtained with the ESO 3.6 m telescope during one complete orbital cycle. Similar to the UV spectra, very pronounced, short-term changes occurred in the emission lines, especially of He II (4686 Å). The analysis of these optical spectra and their correlation to the UV measurements is in progress, and first results look already very promising.

References

- Barnard, E. E.: 1919, *Astrophysical Journal*, **49**, 199.
- Clark, D. H. and Stephenson, F. R.: 1977, "The Historical Supernovae", Pergamon Press, Oxford, New York.
- Drechsel, H., Rahe, J., Holm, A. and Krautter, J.: 1980, *Astronomy and Astrophysics*, submitted for publication.
- Kraft, R. P.: 1964, *Astrophysical Journal*, **139**, 457.
- Mustel, E. R. and Boyarchuk, A. A.: 1970, *Astrophysics and Space Sciences*, **6**, 183.
- Payne-Gaposchkin, C.: 1957, "The Galactic Novae", North-Holland Publ. Company, Amsterdam.
- Rahe, J., Boggess, A., Drechsel, H., Holm, A. V., and Krautter, J.: 1980, *Astronomy and Astrophysics*, Letters, **88**, L9.
- Williams, R. E.: 1980, private communication.

ESO COUNCIL DECISIONS

At its last meeting on November 26, 1980, the ESO Council took a number of decisions; among them we note:

- The approval of the ESO plans to submit a proposal to ESA to host the Space Telescope European Coordinating Facility.
- The approval of the 1981 budget, including 5 million DM for the installation on La Silla of the Max-Planck-Gesellschaft 2.2 m telescope.
- Professor P. Ledoux was elected President of Council from July 1, 1981. Professor J.-F. Denisse will continue as President until that time.
- Mr. H. Grage was elected Chairman of the Finance Committee for the year 1981.
- Professor B. Westerlund was elected Chairman of the Observing Programmes Committee for 1981. Professor Hunger was Chairman of the OPC in 1980.
- Professor P. Lena was reconfirmed as Chairman of the Scientific Technical Committee.
- The inauguration of the ESO Headquarters in Garching will take place on May 5, 1981.

List of Preprints Published at ESO Scientific Group

September—November 1980

118. M. Azzopardi, J. Breysacher and G. Muratorio: Spectroscopy of the Small Magellanic Cloud Emission Line Star Hen S 18. *Astronomy and Astrophysics*, Research Note. October 1980.
119. J. Bergeron, T. Maccacaro and C. Perola: Far UV Study on the Non-thermal Activity in the Narrow Line Galaxies NGC 4507 and NGC 5506. *Astronomy and Astrophysics*. October 1980.
120. L. Martinet and P. Magnenat: Invariant Surfaces and Orbital Behaviour in Dynamical Systems with 3 Degrees of Freedom. *Astronomy and Astrophysics*. October 1980.
121. S. D'Odorico, P. Benvenuti, M. Dennefeld, M.A. Dopita and A. Greve: Astrophysical Interpretation of the $\lambda\lambda$ 1200—7300 Å Emission Line Spectrum of a Filament in the Cygnus Loop Supernova Remnant. *Astronomy and Astrophysics*, Main Journal. November 1980.
122. M.-H. Ulrich: 3C273: A Review of Recent Results. *Space Science Reviews*. November 1980.
123. G. Chincarini, M. Tarenghi and C. Bettis: Observations of Galaxies in the Southern Cluster CA 0340—538. *Astronomy and Astrophysics*. November 1980.
124. R. Schoembs and N. Vogt: High-time Resolution Spectroscopy of VW Hydri and WX Hydri. *Astronomy and Astrophysics*, Main Journal. November 1980.
125. W. Eichendorf, A. Heck, J. Isserstedt, J. Lub, M. Pakull, B. Reipurth and A. M. van Genderen: On the Nature of the 125-day Cepheid V 810 Cen (= HR 4511): IUE Spectra. *Astronomy and Astrophysics*. November 1980.

The Density of the Broad-Line Emission Region in Seyfert 1 Galaxies

M. P. Véron and P. Véron, ESO

One of the characteristics of Seyfert 1 nuclei and quasars is the presence in their spectrum of broad permitted lines or broad wings to the permitted lines. The forbidden lines show no such wings. Because broad He I and He II lines appear in the spectra of quasars and Seyfert 1 galaxies, it seems very likely that ions such as O⁺, O⁺⁺ or Ne⁺⁺ actually do exist in the broad-line region and that the forbidden lines are suppressed by collisional de-excitation in a region with electron densities $N_e > 10^7 - 10^8 \text{ cm}^{-3}$ (Souffrin, 1969, *Astronomy and Astrophysics*, **1**, 305; Anderson 1970, *Astrophysical Journal*, **162**, 743). Some class 1 Seyfert 1 galaxies and low redshift quasars exhibit an anomalously strong He I λ 5876 Å line; this has been believed to show an unusually large helium-to-hydrogen abundance ratio; however, in a high-density nebula, the He I triplet line intensities are significantly enhanced by electron collisional excitation. Theoretical and observational evidence shows that the gas which gives rise to the broad He I lines is characterized by $N_e \sim 5 \times 10^9 \text{ cm}^{-3}$ and $T \sim 15,000^\circ \text{ K}$ with normal abundance (Netzer 1978, *Ap. J.*, **219**, 822; Feldman and MacAlpine 1978, *Ap. J.*, **221**, 486).

On the other hand, the presence of a broad [C III] λ 1909 Å line in the spectrum of almost every QSO where it should be observable sets an upper density limit $N_e \leq 10^{10} \text{ cm}^{-3}$ (Osterbrock 1970, *Ap. J.*, **160**, 25); this line has also been observed in the UV spectrum of the Seyfert 1 galaxy NGC 4151 (Boksenberg et al. 1978, *Nature*, **275**, 404).

It has become customary to assume that the density of the dense region in all quasars and Seyfert 1 nuclei was the same,

in the range $10^{9.5} - 10^{9.6} \text{ cm}^{-3}$. However, both higher and lower values have been suggested; in the case of the QSO Q1011 + 25 (= TON 490) which has a redshift $z = 1.63$, the lines of C III at 977 and 1909 Å have been observed (the first one with the International Ultraviolet Explorer) with an intensity ratio of 1.4 which corresponds to $N_e \sim 19^9 \text{ cm}^{-3}$ if $T_e = 30,000^\circ \text{ K}$ and to $N_e = 3 \times 10^{10} \text{ cm}^{-3}$ if $T_e = 15,000^\circ \text{ K}$ (Nussbaumer and Schild 1979, *Astronomy and Astrophysics*, Letters, **75**, L17).

ANNOUNCEMENT of an ESO Conference in Garching 24–27 March 1981

ESO is organizing a conference on

Scientific Importance of High Angular Resolution at Infrared and Optical Wavelengths

to be held in the ESO building in Garching
on 24–27 March 1981

The Scientific Organizing Committee: M. H. Ulrich,
Chairman—A. Boksenberg—D. Dravins—A. Labeyrie—P.
Léna—G. Weigelt.

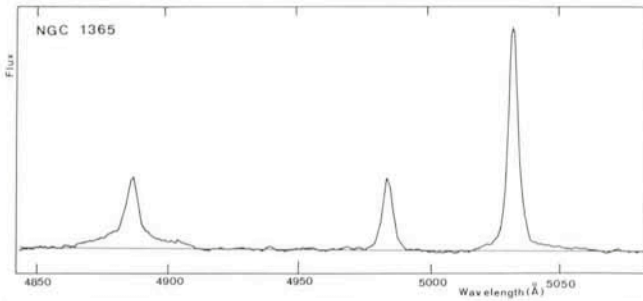


Fig. 1: Spectrum of NGC 1365 obtained with the Boller and Chivens spectrograph and the IDS attached to the ESO 3.6 m telescope. The exposure time was 30 min, the entrance aperture 2 by 4 arcsec. A dispersion of 60 Å/mm was used, which gives a resolution of about 3.2 Å (FWHM). The emission lines shown here are H β and [OIII] $\lambda\lambda$ 4959, 5007.

Most of the spiral Seyfert 1 galaxies have permitted Fe II lines in their spectra but the forbidden [Fe II] lines are usually not observed; if they are suppressed by collisional de-excitation, then $N_e \geq 10^7 \text{ cm}^{-3}$ (Phillips 1978, *Ap. J. Suppl.* **38**, 187). However, both the forbidden and the permitted Fe II lines have been observed in the spectrum of the Seyfert 1 galaxy I Zw 1, which yields to a density $N_e \sim 10^7 \text{ cm}^{-3}$ (Oke and Lauer 1979, *Ap. J.*, **230**, 360).

In the course of a spectroscopic study of the line profile in emission-line galaxies, carried out with the ESO 3.6 m telescope on La Silla, we have found out that, in addition to a broad

H β component, the spectrum of two Seyfert 1 galaxies (NGC 1365 and NGC 7469) show a broad component under the forbidden line [OIII] λ 5007 (Fig. 1). In both cases, the intensity of the broad N2 component is about half of that of the broad H β component. For the narrow components, we have $I(\text{N}2)/I(\text{H}\beta) = 4$ and 6 for NGC 1365 and NGC 7469 respectively. If we made the assumption that the excitation condition in both the low and high density regions are the same, then, in the broad line region, the N2 line is collisionally de-excited by a factor of 8 and 12 respectively.

According to the formula given by Seaton (1975, *M.N.*, **170**, 475), this implies a density of $(1-3) \times 10^6 \text{ cm}^{-3}$ for an electron temperature in the range $T_e = (1-3) \times 10^4 \text{ K}$. In NGC 7469, the [OIII] λ 4363 narrow line is rather strong, being about a tenth of the strength of the narrow component of the [OIII] λ 5007 line, indicating a rather high temperature in the low density region (Wampler 1971, *Ap. J.*, **164**, 1; Anderson 1970, *Ap. J.*, **162**, 743); if the temperature is the same in the high density region, the broad component of the λ 4363 line would be as strong as the λ 5007 line, as, at densities not exceeding $3 \times 10^6 \text{ cm}^{-3}$, the auroral line is not significantly suppressed by collisions.

These observations have shown that the broad emission-line regions of Seyfert 1 galaxies may have densities as low as $\sim 10^6 \text{ cm}^{-3}$, much smaller than previously thought.

We plan to try to detect the auroral line of [OIII] in these two galaxies and to observe more bright Seyfert 1 galaxies to find out if such low densities are common in the broad line regions.

Optical and Ultraviolet Spectroscopy of the Nuclei of Seyfert Galaxies

H. Schleicher and H. W. Yorke, Universitäts-Sternwarte, Göttingen

The launching of the International Ultraviolet Explorer (IUE) in 1978 has made the ultraviolet sky in the wavelength region from 1150 Å to 3200 Å accessible to detailed spectroscopic study. The IUE is a satellite in a geosynchronous orbit, equipped with a 45 cm telescope with two spectrographs. For a more detailed description of this satellite, the interested reader is referred to the article by A. Heck et al. (*Messenger* No. 15, Dec. 1978). Although the diameter of the IUE telescope is quite small—its size is more typical of an amateur telescope than of a scientific instrument—it has been used successfully even for extragalactic spectroscopy.

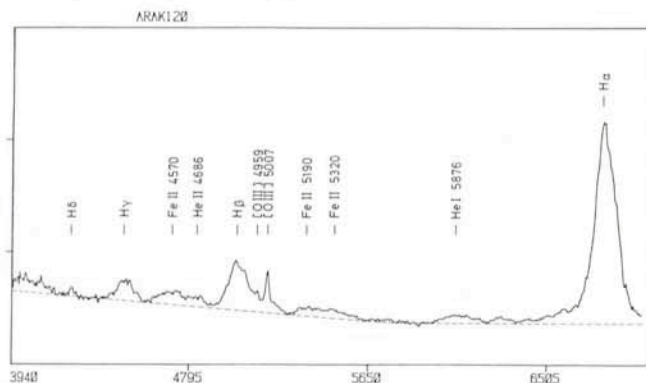


Fig. 1: The optical spectrum of Akn 120, obtained with the IDS. The relative flux is plotted versus observed wavelength. No correction due to galactic extinction has been applied. The dashed line indicates the continuum.

Seyfert Nuclei

The nuclei of Seyfert galaxies have become popular subjects for research, since it was realized that they resemble QSOs in several respects. Seyfert nuclei have smaller redshifts than QSOs; they are much less luminous and are embedded in a clearly visible galactic disk. The optical spectrum of a Seyfert nucleus is dominated by very broad emission lines of the Balmer sequence and by the relatively narrow forbidden lines of [OIII] (in this article we will restrict ourselves to the case of Seyfert 1). Several other broad, but weaker, emission lines seen in Seyferts originate from He I and Fe II. Fig. 1 shows the optical spectrum of Akn 120, which one of us (H. S.) obtained with the IDS at the ESO 3.6 m telescope. Note the asymmetric, bumpy structure of the Balmer lines. The shapes of the permitted lines can be explained by a model in which the gas is confined in clouds or filaments surrounding a central compact source of continuum radiation. These filaments move relative to each other with high velocities. A bump in the H β profile of Akn 120, e.g. 80 Å shortward of line centre, would be produced by filaments which move towards us (relative to the mean velocity of all filaments) with a velocity component of 4800 km/s. Obviously the narrow forbidden lines originate in a different region of the nucleus with much smaller internal velocities ($\leq 600 \text{ km/s}$). Forbidden lines occur only if the electron density is less than $\sim 10^7 \text{ cm}^{-3}$. The absence of broad wings in the [OIII]-lines therefore indicates that the electron density exceeds 10^7 cm^{-3} in the "broad line" filaments.

Unfortunately, not much more information on the physical conditions in the broad line region can be extracted from optical spectra alone. The hydrogen and helium lines are produced mainly by recombination, and their intensities therefore depend only weakly on temperature and densities. Saturation effects complicate their interpretation. The Fe II ion has a rather complex structure and the values of its atomic parameters are very uncertain.

The situation can be improved by including the ultraviolet spectra in the analysis. Here most of the conspicuous lines are produced in transitions from levels 4 to 10 eV above the ground state. Because these lines are generally more sensitive to collisional processes than optical lines, their intensities provide stronger constraints for models of the broad line region.

Observations

In 1978 our group in Göttingen (K. J. Fricke, W. Kollatschny, H. Schleicher, H. W. Yorke) began a programme of observing active galaxies in the optical and UV spectral regions. We first compiled a list of 12 Seyfert galaxies with bright cores suitable for the IUE. This sample included a wide range of intrinsic luminosities and degrees of activity. In our original programme, however, we underestimated the amount of IUE exposure time necessary for a good spectrum, and overestimated the amount of IUE time which we thought would be allotted to us, both by a factor of at least two. The three Seyfert galaxies (NGC 1566, NGC 7603, Akn 120), which we in fact observed with the IUE, were chosen more by accident than by intention. Some objects had to be excluded at the time of observing, because they were too close to the sun, moon or earth. Other objects had already been observed by colleagues in the meantime. As a further constraint, we did not wish to use too much of our allotted IUE time positioning the satellite – under extreme conditions the IUE needs more than two hours to move across the sky over a wide angle.

The IUE observations were made in August and November 1979 in the IUE low spectral resolution mode. Optical observations with the ESO 3.6 m telescope were made in October of the same year. The time differences between UV and optical observations were 70 days and 20 days, a fact which is very important, considering the time variability of these sources. Using the IDS we scanned eight galaxies, including the three galaxies observed with IUE in the wavelength range $\lambda\lambda$ 3940–7200 with a dispersion of 171 Å/mm for a spectral resolution comparable to our UV spectra.

From the viewpoint of a visiting astronomer not intimately familiar with the sophisticated IDS and IUE systems, we were grateful that all technical handling of the apparatus was conducted by skilled observatory staff members. The activity of the visiting astronomers during the measurements is more or less restricted to identifying the objects, specifying the exposure time and occasionally complaining about the poor signal-to-noise ratio.

Results

In the following we will discuss some of the most important features of the spectrum of Akn 120, the strongest of the three sources observed in the UV. The optical and UV spectra are shown in Fig. 1, 2 and 3. The redshift of Akn 120, known to be $z = 0.0325$, can easily be seen in Fig. 3, by comparing the intrinsic Ly α emission line to the non-redshifted geocoronal Ly α line at λ 1216.

Before any further interpretation of these spectra can be made, one has to correct for selective absorption effects caused by dust along the line of sight.

Using 21 cm maps from Burstein and Heiles (1978), we

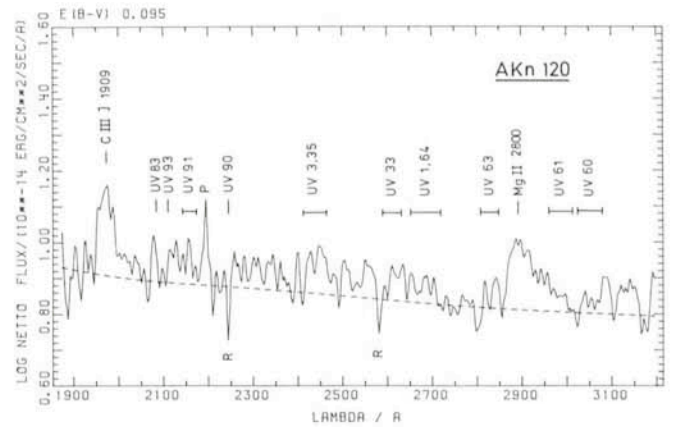


Fig. 2: UV spectrum of Akn 120 obtained with the long wavelength camera of the IUE. The logarithm of absolute flux, corrected for galactic extinction, is plotted versus observed wavelength. Only multiplets of Fe II expected to be strong are indicated. P is a camera blemish, R denotes reseau marks.

estimated the amount of neutral hydrogen and thus the amount of dust in our own galaxy in the direction towards Akn 120. We derived a value of $E(B-V) = 0.095$, which implies a correction of a factor of about 2 for the flux near the Ly α line. The effect of dust within the source itself is much more difficult to estimate. Here, recombination line ratios are useful, because of their weak dependence on temperature and density. Recombination theory predicts a value for He II 1640/He II 4686 of about 7. We measured a line ratio of about 5. However, both lines are blended with other lines (mainly Fe II) and our observed line ratio is therefore uncertain by a factor of 2. We conclude that the amount of dust intrinsic to Akn 120 does not exceed $E(B-V) = 0.15$.

The spectrum of Akn 120 in the wavelength region $\lambda\lambda$ 2700–2800 (see Fig. 2) lacks conspicuous emission lines. However, there are a large number of broad but shallow Fe II lines which overlap and thus form a “pseudo-continuum”. The energy emitted by the Fe II lines in the UV could in fact be as large as a factor of 5 greater than that emitted by the optical Fe II lines.

Correcting for galactic absorption only, we find an intensity ratio Ly α /H β of 10. For the past few years, the intensity ratio Ly α /H β has been under extensive discussion. Prior to the launching of IUE, measurements of high redshift QSOs in the optical (for Ly α) and the infrared (for H β) yielded values between 2 and 5, whereas standard recombination theory

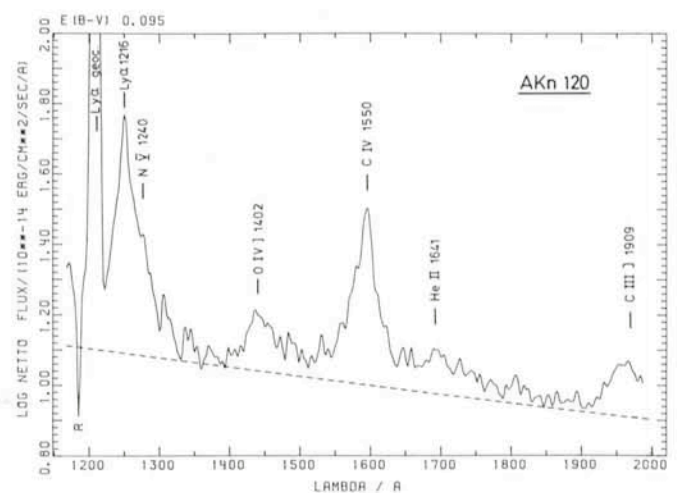


Fig. 3: Same as Fig. 2 for the short wavelength camera of the IUE.

predicts a value around 40. Even when saturation effects in the Balmer lines and collisional processes are taken into account, the expected line ratio is not changed very much. In order to explain this discrepancy, Ferland and Netzer (1979: *Astrophysical Journal*, **228**, 274) have included the effects of internal dust in their calculations and obtain a value $\text{Ly}\alpha/\text{H}\beta = 13$ for internal $E(B-V) = 0.15$. This model is marginally consistent with our results. If Akn 120 were to have no internal dust, however, there would still be a discrepancy of at least a factor of 3 between observation and theory.

Fortunately, the important line ratios $\text{Ly}\alpha/\text{CIV } 1550/\text{HeII } 1640/\text{CIII] } 1909$ are not affected strongly by internal dust as long as $E(B-V) < 0.15$. We have compared our observed values with dust-free model calculations by Davidson and Netzer (1979: *Reviews of Modern Physics*, **51**, 715) and obtain

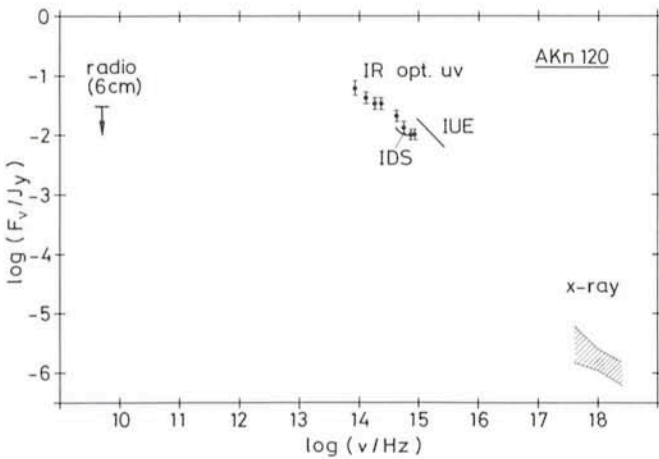


Fig. 4: The overall spectrum of Akn 120, combining observations in various frequency ranges by several authors during 1968 to 1980. At 5 GHz (6 cm), only an upper limit of the flux is known.

a reasonable fit for a certain value of the adjustable parameter U_1 . U_1 is equal to the ratio of the density of incident ionizing photons to the electron density in the broad line filaments. Once a value for U_1 has been fixed, the temperature and ionization stratification within the filament is given. Due to the presence of the CIII] 1909 line, the electron density should be of the order of 10^9 cm^{-3} . The temperature in the region where helium is singly ionized is about 17,000 K. It is possible to estimate the distance of the filaments from the central source of ionizing radiation, if the flux of ionizing photons, the electron density and the value for U_1 are known. Extrapolating the observed UV continuum to wavelengths shortward of the Lyman limit, we estimate the typical distance of the filaments to the central source to be 1 pc. A more realistic model of the broad line region should include tens of thousands of filaments each with a different value for U_1 , depending on its distance from the central source. These filaments would cover about 10% of the sky as seen from the central continuum source.

Very little is known about the nature of the central source which provides the energy radiated away directly in the continuum or indirectly in the emission lines. From the variability of the continuum, its size must be smaller than 30 light days, much smaller than the distance to the broad line producing filaments. Fig. 4 shows the distribution of the continuum over a large range of the electromagnetic spectrum. The continuum decreases from the infrared to the soft X-ray region with an overall spectral index of $\alpha = 1$ ($F_\nu \propto \nu^{-\alpha}$). At 6 GHz the object was weaker than 30 mJy, indicating a cut-off somewhere in the mm or cm wavelength range.

There is a jump of a factor of 2 in the flux between the optical and ultraviolet. Because the optical and UV measurements were made only 20 days apart, it is unlikely that such a jump can be explained by the source's variability alone. Low-redshift QSOs often have a bump in their continuum in the spectral range where this jump occurs in Akn 120. Simultaneous optical and UV measurements of Akn 120 are necessary in order to clarify the situation.

NEW FACILITIES AND IMPROVEMENT OF EXISTING INSTRUMENTATION

Fast Photometry – New Facilities at La Silla

H. Pedersen, ESO

The standard photometric equipment at La Silla has 1 second of time as the shortest integration time. This is fully sufficient for most observing programmes. There are, however, several kinds of phenomena which have timescales of about a second or shorter. Among the fastest phenomena, one could mention the optical outbursts of the X-ray bursters (see *The Messenger* No. **18**, 34) or occultations of stars by objects in the solar system.

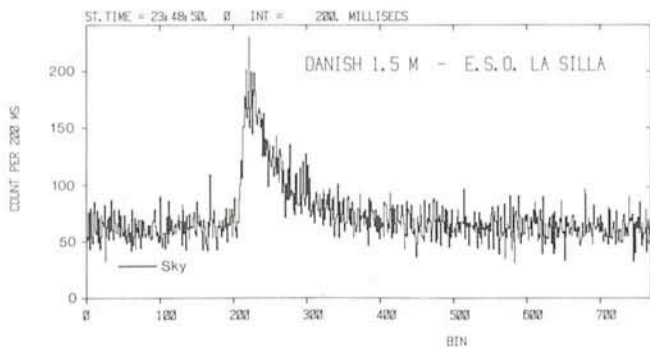
The astronomer who intends to do such observations will normally need to know the absolute time of each single integration, at least to an accuracy corresponding to the duration of the integration. Various computer programmes and pieces of hardware have hitherto been accommodated to the needs of the La Silla observers, but so far, all timing information had to rely on calibrations using radio signals, e.g. the WWV time-signals at 15 kHz.

The availability of an atomic-beam clock on La Silla (*The Messenger* No. **16**, 11) prompted us to design a new set-up for

doing "fast photometry". As soon as the basic principles of operations had been defined, Messrs. D. Hofstadt and F. Gutierrez started programming. Within 10 days they had completed a programme of about 2000 lines of assembler code—without an error. Immediately thereafter, the programme, with its associated hardware, was taken into use both at the 3.6 m and the Danish 1.5 m telescopes.

The fastest data-taking rate is 1 kHz, but any integer multiple of 1 ms can be used as integration time. The photomultipliers interchangingly feed two sets of counters, one set being read while the other is counting. Thereby, the loss of time between two successive integrations can be kept very short—of the order of nanoseconds. Each single integration—from up to four photomultipliers—is written on magnetic tape for later analysis. An on-line pen recorder shows the signal strength in two of the channels. The time resolution of the pen recorder can be selected as any integer multiple of the integration time.

The programme is controlled from a Hewlett Packard terminal. From there, the observer selects integration time and



An example of a typical application of the fast-photometry software. The figure shows an optical outburst of the X-ray burster MXB 1636–53 recorded on July 8, 1980. The burst rises in about 2 seconds to nearly 5 times its pre-burst average. The observation was made in white light at the Danish 1.5 m telescope at La Silla.

starts/stops the data acquisition. Other commands allow changes of the time base and scale parameters for the pen recorder. The observer can also request to be informed about

Pointing of the 3.6 m Telescope

André B. Muller, ESO

The pointing of a telescope on a certain celestial object is achieved when the object is acquired in the field of view of the telescope and on the centre of a cross-wire system or any marking that indicates the centre of this field. Star acquisition with the 3.6 m telescope is computer-controlled. However, the behaviour of the telescope, mainly concerning flexures in the telescope structure, misalignments in the telescope axes and optics, must be known in detail. To find the different contributions to the total pointing error, a pointing programme was developed at the Anglo-Australian Observatory by P. Wallace for the pointing of the Anglo-Australian telescope, and this programme was made available to the author, thanks to Donald Morton, Director of the AAO, and P. Wallace.

The author performed the first pointing tests at the prime focus of the 3.6 m telescope, and the data were reduced at the AAO by P. Wallace, who developed a pointing model for this telescope. Basically, this pointing model is still in use. For some errors, which were discovered in the long run, corrections to the existing ones were added.

Pointing at the Cassegrain focus showed large erratic errors, and it took quite some time to locate the cause. Pointing tests showed a weakness in the support of the Cassegrain mirror, caused by the collimation device. Transducer measurements performed by J. van den Brenk, P. Halleguen and J. van der Ven of the TRS (Technical Research Support) group of ESO-La Silla clearly demonstrated this weakness. It was effectively cured by J. van der Ven, and new tests showed a considerable improvement in pointing.

The pointing programme was implemented in the telescope computer by D. Hofstadt, head of the TRS, and is used for pointing in the prime focus with the Gascoigne corrector and in the Cassegrain focus with any auxiliary equipment.

The programme for the remote control of the triplet adapter in the prime focus does not yet allow the implementation of the pointing programme. However, for the time being, an HP 41 calculator can take care of the pointing with this equipment.

the average of the following N integrations, N being an observer-defined integer.

After the end of the observations, the magnetic tape or selected parts of it can be replayed on a graphic terminal or plotted on an x-y plotter. This can eventually be done at a lower time resolution than used for the observations. The off-line programme, together with similar editing, copying and listing programmes, have been written by Dr. C. Motch. We intend also to write a conversion programme that will transform the data to the FITS format.

So far, the programme has been used with the Behr photometer, the IR photometer and the new general-purpose photometer, all at the 3.6 m telescope and at the Danish 1.5 m with the Roden photometer, the Strömgren photometer and a Danish double-channel photometer. At the two remaining photometric telescopes, the ESO 50 cm and 1 m, the new fast-photometry software cannot be used because of different hardware configurations. When used with the IR and general-purpose photometers at the 3.6 m telescope, the diaphragm and filter wheels have to be set in advance. Later on, however, we intend to merge the fast-photometry programme with the normal photometry programmes, thereby giving the observer full command over the instrument.

Results

Table 1 shows the pointing results of last August 23/24 and 24/25 at the prime focus equipped with the triplet adapter; r being the distance between the centre of the cross wire and the calculated pointing position:

$$r = \sqrt{(\Delta h \cos \delta)^2 + (\Delta \delta)^2}$$

where Δh is the error in hour angle and $\Delta \delta$ the error in declination for the acquired object.

The first line contains the rms errors in r , $\Delta h \cos \delta$ and $\Delta \delta$. The remaining part of the table shows how many stars in quantity and percentage were acquired within 5, 10, 15 and 20 arcseconds. The table shows that the pointing in declination is better than in right ascension.

Table 2 gives the results of the pointing test at the Cassegrain focus last August 27/28. It needs no further explanation. Here again the pointing in declination is better than in right ascension.

Table 1

Prime focus Aug 23/24 + 24/25. 83 objects.

n (83)	$r = 0'' \pm 7''.1$	$\Delta h \cos \delta = 0'' \pm 6''.1$	$\Delta \delta = 0'' \pm 3''.6$
$n \leq 5''$	38 = 45.8%	51 = 61.4%	71 = 85.5%
$n \leq 10''$	74 = 89.2%	78 = 94.0%	83 = 100%
$n \leq 15''$	82 = 98.8%	82 = 98.8%	$-6'' \leq \Delta \delta \leq +8''$
$n \leq 20''$	83 = 100%	83 = 100%	

Table 2

Cassegrain focus Aug 27/28. 53 objects.

n (53)	$r = 0'' \pm 6''.5$	$h \cos \delta = 0'' \pm 6''.4$	$\Delta \delta = 0'' \pm 3''.8$
$n \leq 5''$	30 = 56.6%	41 = 77.4%	46 = 86.8%
$n \leq 10''$	46 = 86.8%	48 = 90.6%	51 = 96.2%
$n \leq 15''$	53 = 100%	53 = 100%	53 = 100%

Conclusion

For prime focus and Cassegrain focus, acquisition of visible objects, as a rule, is better than $10''$. All stars during the above-mentioned tests were acquired within $20''$, covering a sky area 5 hours east to 5 hours west in right ascension and from -85° to $+25^\circ$ in declination.

For invisible objects, a visible pointing calibrator and off-set coordinates for acquisition of the invisible object must be used. The invisible object can then be acquired with an accuracy of ± 1.5 arcsec in right ascension and ± 1 arcsec in declination, which is the resolution of the telescope encoders.

For infrared observations, scanning an area of 10×10 arcsec² will, as a rule, acquire the object. Scanning an area of 20×20 arcsec² may sporadically be necessary.

Off-set may be desirable for very faint objects, where object acquisition may require a long integration time. It goes without argument that off-set coordinates should be calculated in day

time and that the observer knows the coordinates of his object accurately for a certain equinox to enable the calculation of the apparent places.

Future Pointing Investigations

A programme for data reductions has been prepared by K. Teschner, programmer of the TRS. This enables the fast calculation of the telescope coefficients from new pointing data.

A plotting programme to visualize the residual errors is being prepared, which may guide the decisions on pointing improvements. Recently, J. Lub (ESO astronomer) has joined in the pointing activity at the 3.6 m telescope. The limiting pointing accuracy is set by the hysteresis effects of the telescope, to which the reaction arms in right ascension and declination contribute largely, being respectively, ± 7 and ± 5 arcsec.

The ESO 1 m Schmidt Telescope Equipped with a Racine Wedge

André B. Muller, ESO

Since November 1980 a Racine wedge can be used in photometric programmes with the ESO Schmidt telescope.

Optical Data

The wedge has an aperture of 144 mm, a thickness of 10 mm and is made of UBK 7 glass. The effective surface of the Schmidt corrector plate, taking into account the vignetting of the wedge, the plateholder device and the spider arms, is 5745 cm². Therefore, the magnitude difference Δm between direct image and wedge image, taking into account 8% light loss due to the wedge reflection, is 3^{m96} . The magnitude range can be enlarged using diaphragms in front of the wedge. Design and construction of the wedge support were done at La Silla (J. van der Ven and W. Vanhauwaert).

The wedge was optically tested in Geneva (M. Le Luyer and M. Wensveen). The transmission is

30 % at $\lambda = 300$ nm
50 % at $\lambda = 308$ nm
70 % at $\lambda = 318$ nm
90 % at $\lambda = 375$ nm
92 % at $\lambda = 700$ nm

The 8% light loss is due to the reflections at the two uncoated surfaces. The F/D for the wedge beam is 21.2 producing an airy disk at the best focus of 1.5 arcsec diameter at $\lambda = 420$ nm.

The wedge causes a defocusing of 1 mm in the focal plane of the Schmidt telescope which, for $F/D = 21.2$, gives a spread of 47 microns or 3 arcsec. The image is perfect as was found from interferometric tests.

The refracting angle of the wedge is 60 arcsec resulting in an angular separation between the main beam and the wedge beam of $31''$ or about 0.5 mm on the photographic plate.

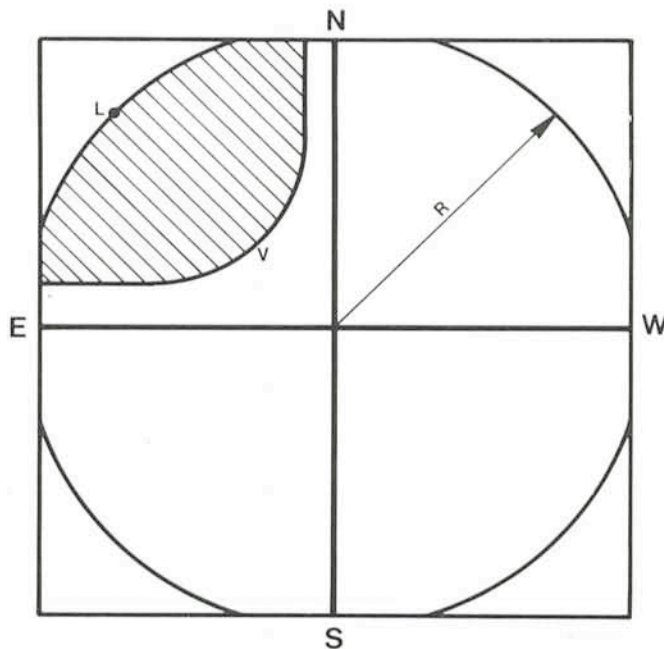
Vignetting

The Racine wedge is mounted directly in front of the corrector plate in the north-east corner. Mounting or demounting the wedge is a matter of minutes.

Although somewhat better vignetting conditions exist by mounting the wedge in the focal plane on the plateholder

device, this possibility was abandoned for reasons of mechanical stability of the plateholder device.

The exposed area of the Schmidt plate is 290×290 mm². The drawing shows the critical radius R of the unvignetted area



of the plate. $R = 154.9$ mm. This means that for stars situated on the circle with this critical radius, the projection of the incident parallel beam is tangent to the circumference of the mirror. Stars outside this circle in the four plate corners are vignetted and cannot be used for photometry without special plate corrections.

The plateholder device and the spider arms obstruct 24.1% of the incident parallel beam. As the dimension of this obstruction is much smaller than that of the corrector plate, its shadow on the mirror is well within the projection of the corrector plate on the mirror. The vignetting due to this obstruction is, there-

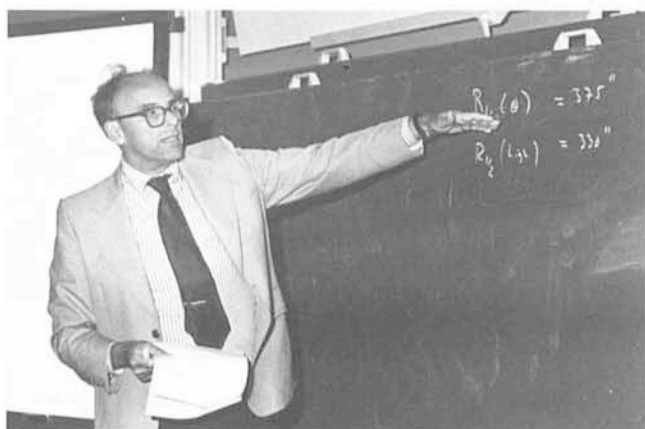
fore, constant within the plate area with radius R and has no photometric consequences. However, the position of this obstruction with respect to the corrector-plate beam is not fixed and moves as a function of the angle of incidence of this beam. As a consequence, in certain directions the plateholder device causes vignetting of the beam passing through the wedge. This

is unavoidable for large-field cameras. The shadowed area in the drawing indicates the area of wedge vignetting. The vignetting starts along the line V and reaches its largest value at point L where it amounts to about 0.5. However, about 85 % of the plate is undisturbed by it. A detailed report on the wedge vignetting is being prepared and will be available within short.

After an interruption of a few weeks, due to the move from Geneva to Garching, scientific life soon started again at ESO. The first seminar took place on October 7; Dr. Sidney van den Bergh from the Dominion Astrophysical Observatory at Victoria, Canada, was talking about "NGC 5128 and its globular clusters".

Después de una interrupción de algunas semanas, debida al traslado de Ginebra a Garching, se ha reanudado la vida científica en ESO. El primer seminario se celebró el 7 de octubre pasado; el doctor Sidney van den Bergh, del Dominion Astrophysical Observatory, en Victoria, Canadá, habló sobre "NGC 5128 y sus cúmulos globulares".

The Image Processing System is working again in the new building.
El Sistema de Tratamiento de Imágenes está de nuevo funcionando, en un edificio nuevo.



ALGUNOS RESUMENES

Cartografía del cielo austral con el telescopio de Schmidt de 1 metro

El "Palomar Observatory Sky Survey" es un medio auxiliar bien conocido y útil para los astrónomos. Todo el cielo del hemisferio Norte está captado en fotografías, cuyas reproducciones se encuentran archivadas en las bibliotecas de casi todos los observatorios importantes del mundo.

Tal colección de fotografías le permite ver al astrónomo qué clase de objetos se hallan en el cielo, y le permite hacer una selección de los objetos que pretende estudiar en detalle.

Dos telescopios se están dedicando ahora a producir un atlas similar del hemisferio celeste austral. Trátase del telescopio de Schmidt del

Reino Unido, instalado en Australia, y del telescopio de Schmidt de 1 metro, instalado en La Silla. La trabajosa tarea se ha repartido de modo que los dos mencionados telescopios están produciendo mapas del cielo de diferentes colores. ESO está elaborando un mapa partiendo de fotografías tomadas en el rojo. El tiempo de exposición para cada placa es de 2 horas, y se tardará unos 5 a 6 años para completar los 606 sectores que cubren el cielo desde la declinación -17.5 hasta el polo celeste Sur. El proceso de producción de las 606 placas originales que se necesitan, y que es preciso copiar para su posterior distribución, es una labor bastante difícil y larga. Cualquier rasguño o mancha en la emulsión, cualquier falta en el revelado, una ruptura de placas, errores de guiado durante la exposición, etc., son ejemplos de las dificultades que pueden presentarse y hacer que una placa sea inservible para la reproducción.

Una tarea igualmente difícil y llena de complicaciones es el proceso de reproducción que se está realizando en Garching, con la finalidad de obtener, de un buen original, copias de buena calidad y en la cantidad

ESO, the European Southern Observatory, was created in 1962 to... establish and operate an astronomical observatory in the southern hemisphere, equipped with powerful instruments, with the aim of furthering and organizing collaboration in astronomy... It is supported by six countries: Belgium, Denmark, France, the Federal Republic of Germany, the Netherlands and Sweden. It now operates the La Silla observatory in the Atacama desert, 600 km north of Santiago de Chile, at 2,400 m altitude, where ten telescopes with apertures up to 3.6 m are presently in operation. The astronomical observations on La Silla are carried out by visiting astronomers – mainly from the member countries – and, to some extent, by ESO staff astronomers, often in collaboration with the former. The ESO Headquarters in Europe are located in Garching, near Munich. ESO has about 120 international staff members in Europe and Chile and about 150 local staff members in Santiago and on La Silla. In addition, there are a number of fellows and scientific associates.

The ESO MESSENGER is published four times a year: in March, June, September and December. It is distributed free to ESO personnel and others interested in astronomy. The text of any article may be reprinted if credit is given to ESO. Copies of most illustrations are available to editors without charge.

Editor: Philippe Véron
 Technical editor: Kurt Kjær

EUROPEAN
 SOUTHERN OBSERVATORY
 Karl-Schwarzschild-Str. 2
 D-8046 Garching b. München
 Fed. Rep. of Germany
 Tel. (089) 320 06-0
 Telex 05-28 282-0 es d

Printed by Universitätsdruckerei
 Dr. C. Wolf & Sohn
 Heidemannstraße 166
 8000 München 45
 Fed. Rep. of Germany

que se necesite. Afortunadamente, ESO estuvo en condiciones de reunir una valiosa práctica en la elaboración de mapas antes de dedicarse al mencionado atlas de fotografías tomadas en luz roja. ESO ya se había dedicado durante varios años a la realización de un atlas del cielo austral con imágenes captadas en luz azul.

Este atlas, llamado "Quick Blue Survey" (QBS), se completó hace aproximadamente

año y medio, y ya se ha distribuido a muchos observatorios de países miembros de ESO, y de otros países.

Con un contenido de muchos miles de objetos, este catálogo y las fotografías de la esfera celeste que se están tomando en Chile y en Australia son el fundamento para futuros programas de fotometría y espectrografía a que se dedicarán los grandes telescopios actualmente instalados en el hemisferio Sur.

NUEVAS POSIBILIDADES Y PERFECCIONAMIENTO DE LOS INSTRUMENTOS

Enfocamiento del telescopio de 3,6 metros

Por algún tiempo, se presentaron problemas para enfocar con precisión el telescopio de 3,6 metros. En los controles realizados por el doctor A. Muller en el foco de Cassegrain, se comprobaron errores considerables, presentándose sin regularidad determinada, causados por una debilidad del soporte del espejo secundario, debilidad que se ha podido remediar ahora. Los errores sistemáticos procedentes de la estructura mecánica del telescopio, fueron medidos y neutralizados con ayuda de un programa desarrollado por el doctor P. Wallace, del Anglo-Australian Observatory. Un programa de enfocamiento en el que se tienen en consideración estos errores, ha sido mejorado por D. Hofstadt, permitiendo ahora enfocar el telescopio hacia todo objeto celeste con una exactitud de aproximadamente 5 segundos de arco, exactitud que se considerará satisfactoria por la mayoría de los astrónomos, exceptuando acaso a los que se dediquen a observaciones en ondas de infrarrojo.

Fotometría rápida en La Silla

Los señores D. Hofstadt y F. Gutiérrez, de ESO en La Silla, han desarrollado un nuevo programa de computador para la fotometría rápida. Este programa ya se está aplicando, con su correspondiente equipo de aparatos

auxiliares, en el telescopio de ESO de 3,6 metros y en el telescopio danés de 1,5 metros. La nueva instalación resultará en particular ventajosa para la observación de fenómenos que se producen en fracciones de tiempo de un segundo o menos, como, por ejemplo, erupciones ópticas de fuentes de rayos X, u ocultaciones de astros por objetos del sistema solar.

El telescopio de Schmidt de 1 metro, equipado con un prisma de Racine

Uno de los más difíciles problemas a resolver por los observadores es la determinación exacta de la magnitud de estrellas débiles. Entre las soluciones que se ofrecen para resolverlo, está el uso del prisma de Racine que, instalado enfrente de la lente de corrección del telescopio de Schmidt, produce de cada estrella una imagen secundaria, en 4 magnitudes más débil que la imagen principal. Comparando la imagen principal de estrellas débiles, por una parte, con la imagen secundaria de estrellas más brillantes y de magnitud conocida, por otra parte, se ha encontrado una posibilidad para ampliar la serie de estrellas de referencia, en un grado de 4 magnitudes. No cabe duda de que muchos de los observadores que se ven en la necesidad de determinar la magnitud de estrellas débiles en las placas de Schmidt, se servirán de este complemento, disponible desde el mes de noviembre pasado.

Contents

J. Audouze, M. Dennefeld and D. Kunth: The Dwarf Blue Compact Galaxies	1
Tentative Time-table of Council Sessions and Committee Meetings in 1981	3
Personnel Movements	4
C.-I. Lagerkvist: Physical Studies of Asteroids – an Observing Programme at ESO	5
H.-E. Schuster: Mapping the Southern Sky with the ESO 1 m Schmidt Telescope	7
Announcement of an ESO/ESA Workshop on "Optical Jets in Galaxies"	7
H. Drechsel, J. Rahe, A. Holm and J. Krautter: Simultaneous Optical and Satellite Observations Provide New Understanding of a Famous Nova	10
ESO Council Decisions	13
List of Preprints Published at ESO Scientific Group	13
M. P. Véron and P. Véron: The Density of the Broad-Line Emission Region in Seyfert 1 Galaxies	13
Announcement of an ESO Conference on the "Scientific Importance of High Angular Resolution at Infrared and Optical Wavelengths	13
H. Schleicher and H. W. Yorke: Optical and Ultraviolet Spectroscopy of the Nuclei of Seyfert Galaxies	14
H. Pedersen: Fast Photometry – New Facilities at La Silla	16
A. B. Muller: Pointing of the 3.6 m Telescope	17
A. B. Muller: The ESO 1 m Schmidt Telescope Equipped with a Racine Wedge	18
Algunos Resúmenes	19